POLITECNICO DI TORINO

Master's Degree in Biomedical Engineering

Master Thesis

carried out in collaboration with

Universitat Pompeu Fabra (UPF), Barcelona

"Identification of statistical critical area of proximal femur when a lateral fall happens"

Internal Tutor

Prof. Lorenzo Peroni

Supervisor

Prof. Simone Tassani

Co-supervisor

Prof. Carlos Ruiz Wills

Candidate

Nicole Morando

2020/2021

A Daniela e Giuseppe,

i miei genitori…

Index of contents

Index of figures

Index of tables

Abstract

Osteoporotic hip fracture is considered a worldwide health problem in the elderly population, with a negative social and economic impact characterized by an increase of hospital cost and a worsening of quality of life.

Diagnostic tools widely used for assessment of osteoporosis include Dual-energy X-ray absorptiometry (DXA), Quantitative Computed Tomography (QCT), FRAX. Although DXA is the gold standard for osteoporosis diagnose, it is not enough reliable for fracture prediction. For this reason, the Finite Element (FE) model rises as a complementary tool to tackle the fracture prediction. In this sense, the evaluation of critical fracture regions on FE model, is often based on visual identification of mapped field introducing under/over estimation of the local nature of fracture event.

The present thesis provides an innovative rigorous methodology applied on FE proximal femur models generated from DXA images, to identify statistically significant difference between fracture and non-fracture group through the application of Random Field Theory (RFT) and its topological extension of statistical process based on Statistical Parametric Map (SPM). The “spm1d” software has been used to compute statistical tests.

The investigated groups include 111 osteoporotic subjects: 62 fractured patients and 49 controls. Fracture region (neck/trochanter), type of tissue (trabecular/cortical) and gender (female/male) were considered in the analyses (Two-sample t-test and Two-way ANOVA with repeated measures) to explore the impact of these factors on the dependent variables Major Principal Stress (MPS) and Major Principal Strain (MPE) obtained by FE simulations. In particular, the significant elements of FE model detected by performing the Two-sample t-test, are implicated in the second level of analysis to take into consideration the interaction between factors.

The results showed the variable MPS as the main significant parameter to discriminate the investigated groups. In relation to the zone detected as statistically significant, it was observed that not necessarily corresponds to the fracture region.

In addition, the elements of the FE model belonging to the regions identified as critical represent only a tiny percentage of neck/trochanter area.

To verify the reliability of this method of analysis, a comparison between the classification made considering actual data belonging to a reduction of neck and trochanter region and one more conservative, that consider all elements of neck and trochanter was performed. The results obtained demonstrate an improvement of predictive power when a reduction of critical regions is considered, reaching a 79% and 89% in the classification of neck and trochanter fracture, respectively.

The implications of these findings suggest an important advance: on one hand in clinical practice, about prevention and early diagnosis and, on the other hand, in biomechanical field concerning the bone behaviour in relation to the event of hip osteoporotic fracture.

1 Introduction

The osteoporotic hip fracture represents a great social and economic burden in developed countries **[1]**. The fractures are often associated with physical disability, reduction of quality of life and increased mortality. In addition, the incidence of osteoporotic hip fracture provides an evident impact on health care cost for pre and post fractures treatments resulting in more days spent in hospital than many other diseases. Because the incidence of osteoporotic hip fracture is closely related to the growth of elderly population, the identification of rigorous statistical methodology for prevention, early diagnosis, appropriate treatment, and classification of hip fractures constitutes an important clinical aim.

1.1 Proximal femur

1.1.1 Bone tissue

The bone tissue is a mineralized and viscous-elastic connective tissue characterized by the capacity to remodel his structure in response to mechanical and organic stimuli. It consists of specific cells and extracellular matrix. The extracellular matrix is characterized by an organic fibrous component of collagen proteoglycans, glycoproteins and by an inorganic amorphous substance.

In the bone tissue it's possible to distinguish an inorganic and organic structure (Fig. 1). The inorganic part is composed of mineral salts such as calcium, magnesium, phosphates and salt citrates giving stiffness and hardness. The principal inorganic component is hydroxyapatite, $Ca_{10}(PO_4)_6(OH)_2$, a mineral composed of calcium phosphate that, in the form of elongated crystals, is arranged in an orderly manner along the collagen fibers. The organic part is composed of osteogenic cells, osteoclasts, osteoblasts, osteocytes and bone lining cells which provide for the growth, production and resorption of bone tissue. Collagen fibers are the main organic components and are responsible for the elastic and viscoelastic behaviour and strength of the bone. The collagen has a triple helix structure based on woven fibers with high tensile strength. The fundamental units of collagen are the fibrils, aggregates of fibrils form fibers, arranged in bundles organized in lamellae of collagen.

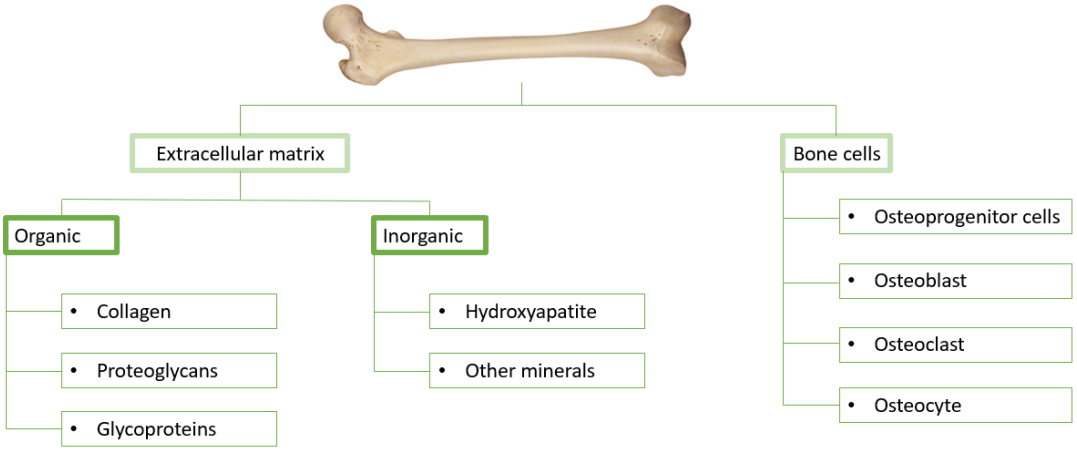

Figure 1: Bone Tissue: organic and inorganic component

The spatial organization of lamellae and apatite crystals allows to distinguish trabecular bone from cortical bone. Cortical bone consists of closely packed osteons with a central canal (haversian canal) surrounded by concentric rings of lamellae of matrix obtaining cylindrical osteons. Between the rings of the matrix, the bone cells (osteocytes) are located in spaces called lacunae. The osteonic (Haversian) canals contain blood vessels interconnected, by perforating canals, with vessels on the surface of the bone.

Trabecular bone is less dense than cortical bone and consists of overlapping lamellae of collagen to obtain a trabecular structure able to follow the stress lines to which the bone is subjected. Trabecular bone, like cortical bone, is supplied but through the porosity between its trabeculae.

1.1.2 Anatomy and structure of the proximal femur

Fig. 2 shows the structure of the femur: external surface is covered by a dense connective membrane of woven fibers (periosteum) inside which blood vessels flow. The internal surface of the bone, instead, is covered by a floor cells membrane (endosteum) with a great osteogenic capacity.

In particular, proximal femur consists of a body (diaphysis), formed by a layer of cortical bone and a wide medullary cavity containing the bone marrow for the production of blood cells, and two extremities (epiphysis) of trabecular bone

covered by a thin layer of cortical bone. Proximally, the femur articulates with the pelvic bone. Distally, it interacts with the patella and the proximal aspect of the tibia.

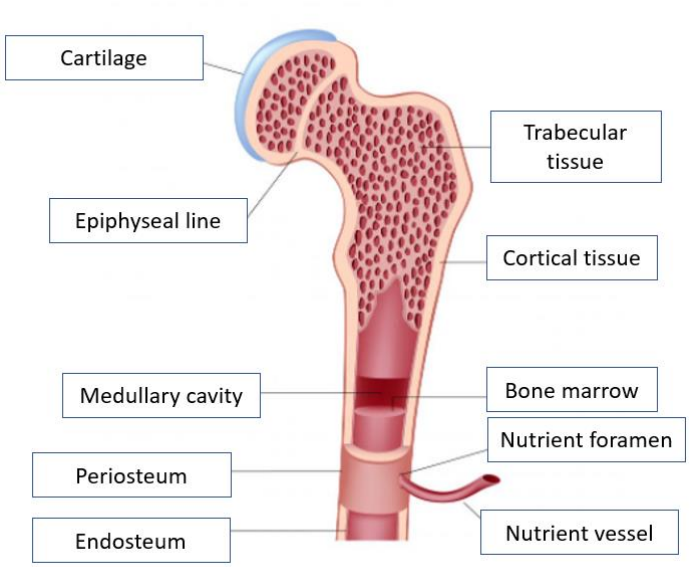

Figure 2: Proximal femur composition

Proximal femur includes the femoral head, neck and the region 5 cm distal to the lesser trochanter (Fig. 3). There is a 125°-130° inclination angle between the head and neck and the femoral body **[2]**.

- **Head** - it links with the acetabulum of the pelvis to form the hip joint. It has a smooth surface, covered with articular cartilage.
- **Neck** - it connects the head of the femur with the shaft. It is cylindrical, projecting in a superior and medial direction.
- **Intertrochanteric area** - it is distal to the femoral neck and proximal to the femoral shaft; it is the area of the femoral trochanters, the lesser and the greater trochanters.
- **Greater trochanter** - it is located at the junction between the neck and the shaft of the femur bone. It is the point of insertion of different muscles: gluteus

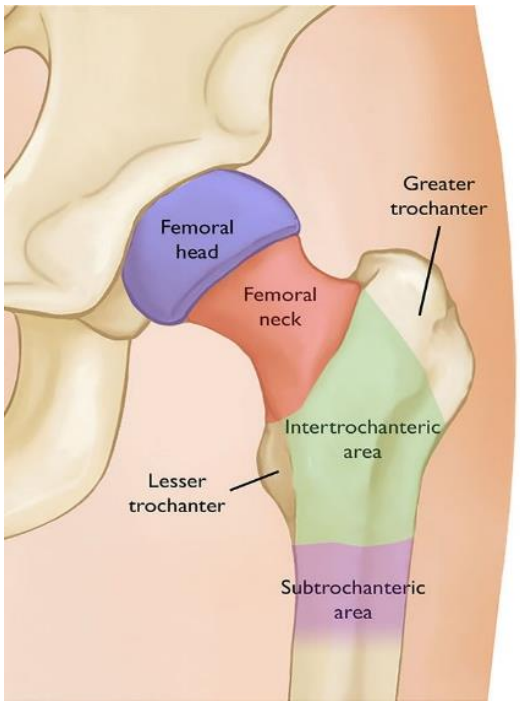

Figure 3: Proximal femur structure

medius and minimus, piriformis, obturator internus and externus, and gemelli muscles.

- **Lesser trochanter** - it projects from the lower and back part of the base of the neck. It receives the insertion of the psoas major and iliopsoas muscles.
- **Subtrochanteric area** - it is the region between the lesser trochanter up to 5 cm below that (distally).

1.1.3 Osteoporotic hip fractures

Osteoporosis is a global health problem whose importance is going to increase with the aging of the population. It is defined as a systemic disorder of the skeleton characterised by low bone mass and deterioration of the microarchitecture of bone tissue, with the consequent increase in bone fragility and the greater susceptibility to fractures **[3]** (Fig. 4).

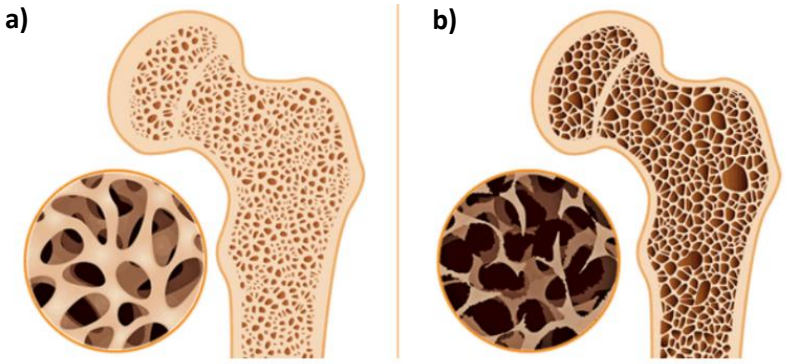

Figure 4:

a) Healthy Bone *b) Osteoporotic bone*

It is possible to distinguish two types of osteoporosis: Primary and secondary osteoporosis.

- **Primary osteoporosis** is in turn divided in *Type I* and *Type II* osteoporosis. The first is associated with a decreased production of estrogen and, to a lesser extent, to testosterone deficiency. It is also called postmenopausal osteoporosis and therefore is largely observed in female during the age of 50-70 **[4].**

While the Type II is related to an increase in age involving both men and women, typically after the age of 70. It is also known as senile osteoporosis.

- **Secondary osteoporosis** is due to the presence of other diseases, medications and certain lifestyle behaviour **[4].**

1.1.3.1 Fracture risk

There are many factors that may affect the onset of osteoporosis increasing the risk of fractures. They can be divided into two main classes: non modifiable factors and potentially modifiable factors.

- **Non modifiable factors**
    - **Age** - Older people are the category most at risk. Around 75% of fractures occur to people aged 65 and over.
    - **Gender** - Women are four times likely to suffer from osteoporosis than men. The cause is due to a lowering of the level of estrogen during and after menopause, the effect of which is the decrease of bone loss.
    - **Ethnicity** - Asian and Caucasian people are at higher risk of developing osteoporosis.
    - **Heredity** - Family history of bone disease may increase the risk of hip fracture.
    - **Body weight** - A decrease in body mass index (BMI) causes a negative impact on bone density and therefore the unavoidable weakening of bone tissue.
    - **Previous fractures** - The presence of previous fractures may represent potential points of initiation of fractures.

- **Potentially modifiable factors**
    - **Lifestyle factors** - Smoking, caffeine, alcohol intake, unbalanced diet, and lack of physical activity increase fracture risk **[5]**.
    - **Vitamin D deficiency** - High levels of vitamin D assist the body to absorb the right amount of calcium by slowing down the development of osteoporosis.

1.1.3.2 Hip fracture classification

Hip fracture is a partial or complete break of the proximal femur. By the ‘’Muller AO Classification of fractures’’ hip fractures are classified according to their anatomical location in two categories (Fig. 5):

- **Intracapsular**
  - Femoral head
  - Femoral neck
    - Sub-capital
    - Trans-cervical
    - Basi-cervical

In Intracapsular regions cortical bone mass is reduced compared to extracapsular regions. It leads to a cortical thinning and a decrease in the density of the cortical bone **[6]**.

a)

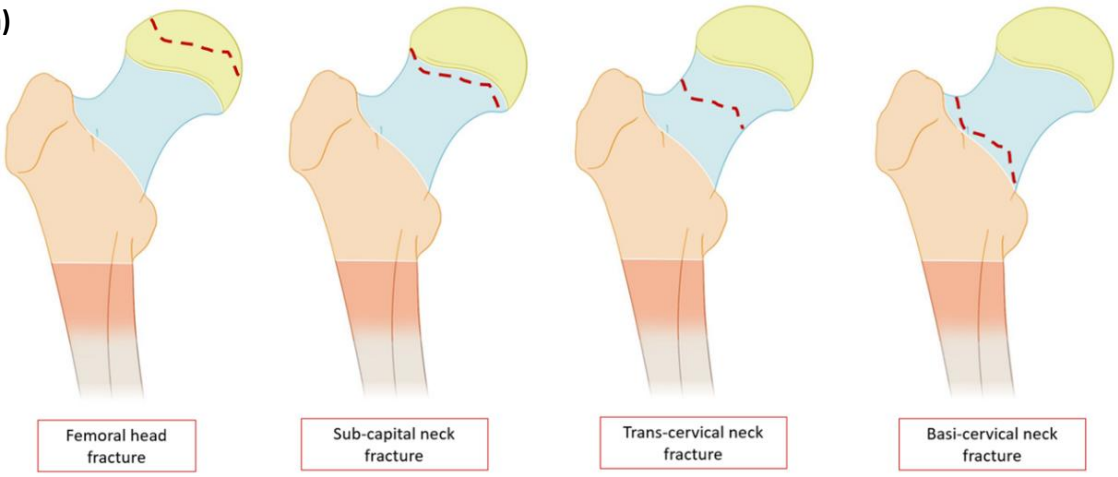

Figure 5:

a) Intracapsular hip fractures classification

- **Extracapsular**
  - Trochanteric
  - Trans-trochanteric
  - Sub-trochanteric

Extracapsular regions contain a large amount of cancellous bone and an adequate blood supply, which makes fractures in this region less susceptible to necrosis intracapsular fractures **[7]**.

b)

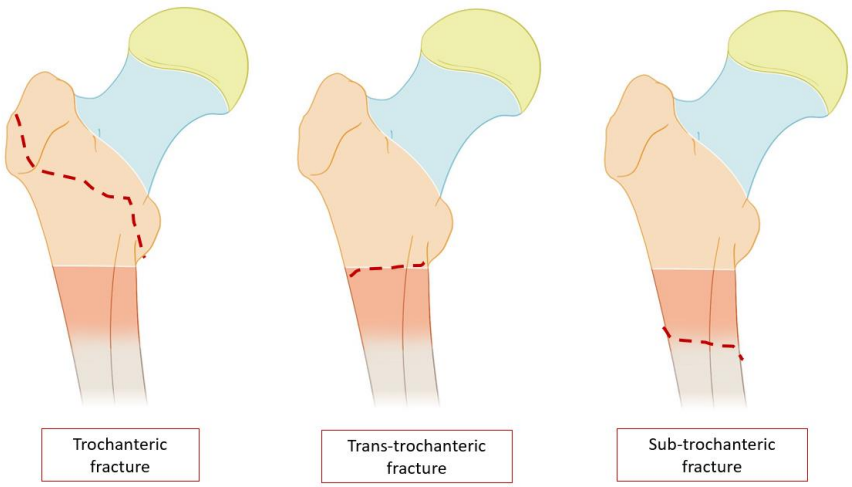

Figure 6:

b) Extracapsular hip fractures classification

1.1.3.3 Epidemiology

According to the International Osteoporosis Foundation (IOF), approximately 22 million women and 5.5 million men aged between 50-84 years are estimated to have osteoporosis in the European Union (EU). Due to changes in population demography the number of men and women with osteoporosis in the EU will rise from 27.5 million in 2010 to 33.9 million in 2025, corresponding to an increase of 23% **[8]**. The number of new fractures in 2010 in the EU was estimated at 3.5 million, comprising approximately 620,000 hip fractures, which represent the most frequent type of fracture followed by forearm fracture (560,000), vertebral fractures (520,000) and other fractures such us clavicle, scapula, pelvis, rib, humerus, tibia **[9]**.

Hip fractures are associated with increased mortality and morbidity; 12% to 17% of patients with a hip fracture die within the first year, and the long-term increased risk of death is twofold **[10] [11]**. Of the patients who survive, only one-half walk independently again, and 20% must move to a long-term care facility **[12]**.

The economic burden of incident and prior fragility fractures was estimated at € 37 billion. Incident fractures represented 66% of this cost, long-term fracture care 29% and pharmacological prevention 5%. The costs are expected to increase by 25% in 2025 **[8]**.

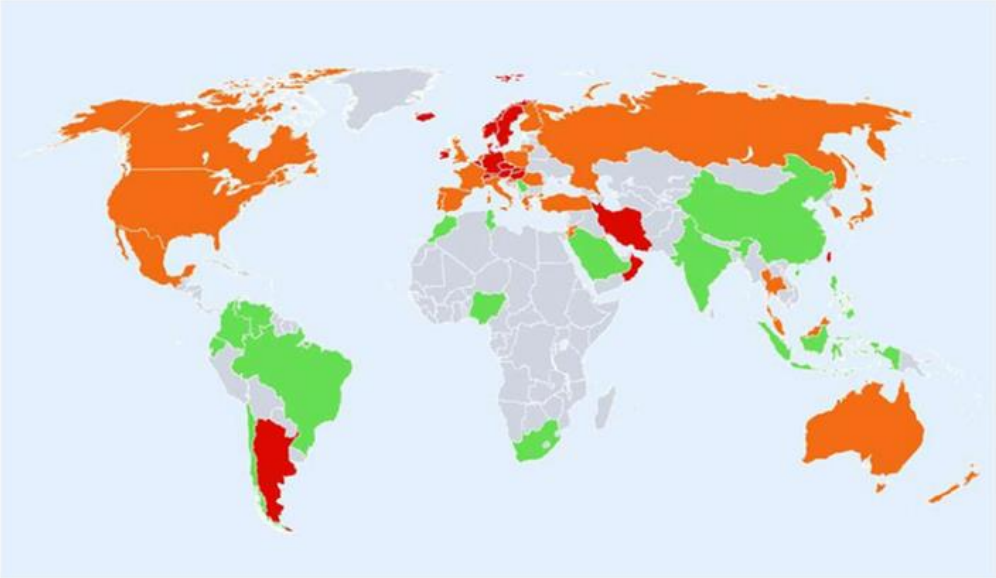

Figure 7: Hip fracture rates for men and women combined in different countries of the world categorised by risk. Where estimates are available, countries are coloured in red (annual incidence >250/100,000), orange (150-250/100,000) or green (<150/100,000) ***[13]****.*

1.2 Random Field Theory

1.2.1 Multiple comparison problem

In statistical analysis the *null hypothesis* (H_0) testing represents a formal approach to study the relationship between two population parameters. If the null hypothesis is verified it means that there is no effect between two variables. If the null hypothesis is rejected, we accept the *alternative hypothesis* (H_1), and it is possible to conclude there is a statistically significant difference between two variables. In rejecting the null hypothesis, we must accept a certain percentage (usually 5%) of error. This is called *Type I error* or α value.

Multiple comparison problem occurs when the statistical analysis involves a large set of statistical tests simultaneously. This state increases the *family wise error rate* (FWER) that is the probability that one or more values will be greater than alpha (P^{FWE}) **[14]**. In other worlds is the probability to reject H_0 when the null hypothesis is true and therefore the probability of incurring false positives.

$$P^{FWE} = 1 - (1 - \alpha_{\{per\ comparison\}})^m \quad [1]$$

Where m represents the independent observation and the reported expression

$(1 - \alpha_{\{per\ comparison\}})^m$ the probability that all tests being less than α.

The equation of P^{FWE} , because α is small, can be approximated with the following expression:

$$P^{FWE} \leq m\alpha \quad [2]$$

1.2.2 Bonferroni correction

There are many strategies to control the false discovery rate, one of the most common is the Bonferroni correction. It adjusts the α value for an individual test dividing P^{FWE} by the number of statistical tests conducted m:

$$\alpha = \frac{P^{FWE}}{m} \quad [3]$$

Because Bonferroni correction expects independent comparisons, it represents a proper procedure, giving a corrected *p-value,* only if there is no correlation between neighbouring statistical values. However, it can be considered too conservative if such independence is not guaranteed. Therefore, the application of Bonferroni correction, for a large number of tests, comes at the cost of increasing the probability of producing false negatives, *Type II error*, reducing statistical power **[14]**.

1.2.3 Alternative solution: Random Field Theory

Random Field Theory (RFT) is a branch of mathematics used to solve the multiple comparison problem. It provides a method for *correcting p-value*, that considers the fact that neighbouring statistical values are not independent, by virtue of continuity in the original data (spatial correlation) belonging to the search volume.

Random Field Theory takes the multiple comparison problem from the context of discrete to the context of continuous pushing the limits of Bonferroni correction (Fig. 7). It follows that RFT is less conservative and much more sensitive, finding a lower threshold which gives the FWER **[14]**.

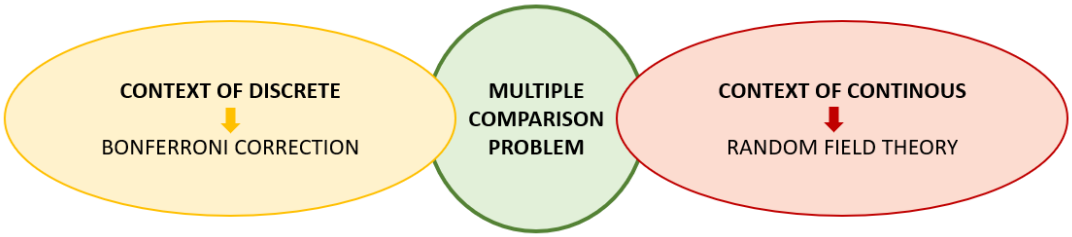

Figure 8: Multiple comparison problem in relation to Bonferroni correction and Random Field Theory

1.2.3.1 Application of Random Field Theory

The application of RFT can be divided in three different steps:

1. **Estimation of the smoothness** (spatial correlation) - The smoothness has the effect of blurring data, reducing the number of independent observations. Because it is unknown the extent of spatial correlation before smoothing, the smoothness can be calculated using the residual values from the statistical analysis described in **[15]** and **[16]**.

   The smoothness can be expressed as the width of a Gaussian kernel used to smooth the data, known as "*Full width of half maximum* (FWHM)". It is a way to consider the search volume in terms of "*resolution elements* (Resels)" in the statistical map **[17]**.

V= volume of the search region;
FWHM= effective Full width at half maximum of a Gaussian kernel used to smooth the data;
D= number of dimensions in the search region.

$$Resels_D = \frac{V}{FWHM^D} \qquad [4]$$

Fig. 8 shows the FWHM defined as the distance between two values of the independent variable at which the independent variable is equal to half of its maximum value.

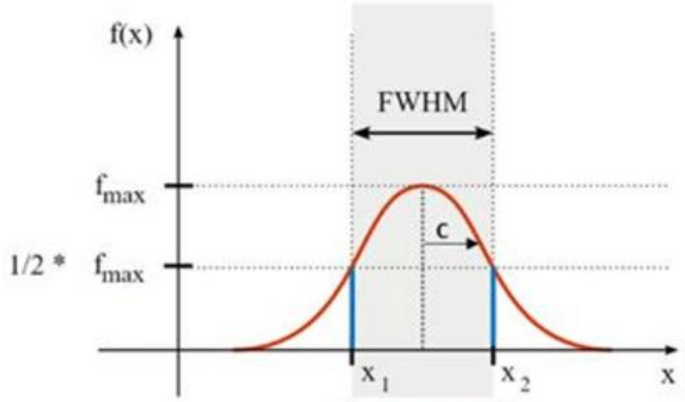

Figure 9: Full width of half maximum (FWHM)

2. **Use the smoothness to calculate the expected Euler characteristic E[EC] at different thresholds** - The expected Euler characteristic corresponds to the probability of finding an above threshold region in a smooth Gaussian field and therefore approximately associated to the probability of a family wise error E[EC]≈ P^{FWE} **[18]**. Consequently, a higher threshold provides a reduction of supra-threshold regions (Fig. 9).

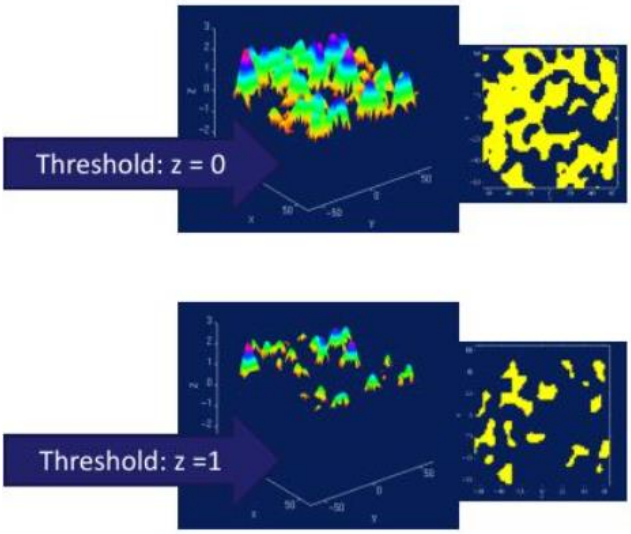

Figure 10: Different threshold value in the same field

EC = Euler characteristic
v = degrees of freedom
z = height of threshold

$$EC(z) = \frac{(4\,log_e)^{\frac{3}{2}}}{(2\pi)^2} + \left(\frac{v-1}{v}z^2 - 1\right)\left(1 + \frac{z^2}{v}\right)^{-\frac{1}{2}(v-1)} \qquad [5]$$

3. **Use the EC to calculate a proper threshold** - The EC previously obtained allows to calculate a proper threshold, which let us reject the null hypothesis erroneously with probability of α, specified by the user. At the end of this procedure a list of probability p-values, one for each threshold-surviving cluster, is obtained.

1.3 State of the art: diagnostic tools for assessment of osteoporosis and fracture risk

The onset of osteoporosis is closely related to bone density loss, causing the weakening of the bone, and making it more susceptible to the fracture risk. Several techniques are commonly used by clinicians to measure the amount of mineral content (BMC) and density (BMD) in the bone **[19]**.

- **Dual-energy X-ray absorptiometry (DXA)** is the most widely used technique to detect osteoporosis because it is easy, quick, and presents a minimal invasive procedure. The amount of radiation dose used is extremely small, reason why this exam can be repeated several times. Nevertheless, because DXA calculates the areal BMD area and not the volumetric BMD the results refer to an estimation of real bone mineral density although a partial correction can be obtained by some mathematical formulas.

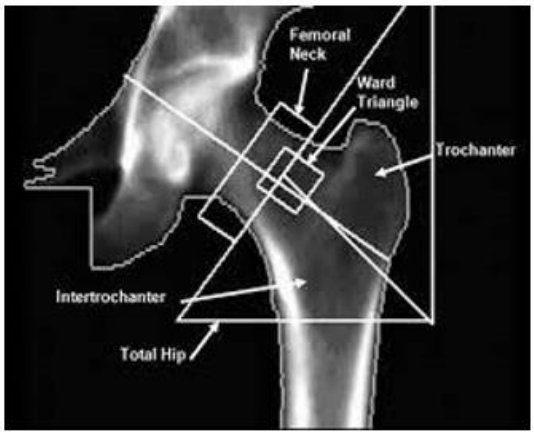

Figure 11: DXA image of proximal femur

  It means that the differences between volumetric and areal bone mineral density should be taken into consideration **[20]**. Despite its limitations, DXA is considered the gold standard tool for diagnosing osteoporosis (Fig. 10).

- **Quantitative computed tomography (QCT)** provides a method to assess osteoporosis in relation to a direct volumetric BMD measurement considering the three dimensions about the spatial location concerning the highly responsive trabecular bone and less responsive cortical bone **[21]**.

Compared with DXA, the QCT technology uses a higher dose of radiation therefore it cannot be used as a routine diagnostic tool. It is also less available for clinicians and expensive.

- **Quantitative ultrasound (QUS)** is a relatively simple procedure, non-invasive and free of side effects. It does not use ionizing radiation, but ultrasound. Despite these advantages, its diagnostic power is much lower than that of DXA and QCT.

- Further methodologies, like **Fracture Risk Assessment Tool (FRAX)** and **bone metabolic markers**, are usually combined with the measurement of bone mineral density for the prediction of fractures based on clinical risk factors and monitoring the bone quality identifying patients with high fracture risk respectively **[22]**. The greater limitation of the FRAX algorithm is represented by the lack of adaptation to patients with rapid bone loss and by the exclusion of many clinical factors available to the specialist and which should be considered for the treatments of osteoporotic patients **[23]**.

- Another advance is the **Finite Element (FE) method** based on DXA images to study mechanical behaviour of bone improving the prediction of fracture risk. In fact, the assessment of osteoporosis based only on DXA suffer of lack sensitivity and was found patients who have suffered from hip fractures, even though they had low values of BMD **[24]**. In this sense, the FE model allows to take into consideration other factors as the geometry, material and mechanical properties and also the boundary conditions. Therefore, the 3D shape reconstruction and BMD distribution starting from 2D DXA images provide an accurate method to achieve patient-specific simulations for the assessment of bone strength under appropriate loading conditions known to cause fractures **[25]**. For this reason, FE model can be considered a complementary tool to DXA to diagnose osteoporosis.
  Also QCT is used in combination with FE model to estimate femoral strength. It is widely employed clinical study to evaluate the influence of factors as age and gender between investigated groups **[26] [27]** and also to analyse the effect of drug therapy for the treatment of osteoporosis **[28]**. By contrast, DXA-based on FE models have not been evaluate in clinical studies as deeper as QCT models. But the fact that QCT uses a higher dose of radiation, and its cost is greater than DXA technology leads us to

believe that it represents a powerful tool especially in research while in clinical settings DXA-based FE analysis will remain the preferred technology **[29]**.

1.3.1 Context of the study and aim of the thesis

Despite DXA-based FE model brings with it the advantages of minimal invasive procedure for the purpose of evaluating not only tissue condition but also biomechanical descriptors obtained from simulation, the identification of the critical region suffers from several limitations.

The selection of statistically different areas between investigated groups concerning the proximal femur is often based on visual identification of mapped field, introducing consequently an under/over estimation of the critical regions belonging to the FE femur model. It would not be correct to consider only the regions with maximum stress and maximum strain as the main critical areas with statistical difference since these regions and values might be only partially related to the development of the fracture **[30]**. Moreover, only a portion of them or regions with lower value of maximum stress and strain may be significant. In addition, there is no reason to assume that these regions, visually identified, are related with the identification of fracture zones and consequently with the initiation zone of the fracture **[30]**. By virtue of the local event of the fracture **[31]**, not all the search volume (proximal femur), takes part to the fragile fracture event, and replace stress/strain values with the value of the mean would be inappropriate, although it is not possible to exclude that surrounded areas, far from the fracture line, are not significant and might actually be determinant in driving the development of the fracture in other regions. For these reasons, the visual identification of FE femur model, does not represent a reliable criterion to discriminate different critical regions between investigated osteoporotic groups.

The aim of the present thesis is the identification of a rigorous methodology based on statistical analysis to automatically identify regions with statistical differences between two groups (fractured and controls) in order to obtain an accurate investigative tool characterized by a general power in clinical setting with a large-scale application.

Random Field Theory (RFT), and its topological extension based on Statistical parametric Map (SPM), will be the mathematics behind the methodology to solve the multiple comparison problem taking into account the correlation between nearby elements in the FE model, spatially related due to the physiological nature of the signal. This approach, based on RFT, lead us to overcome the known limitation due to Bonferroni correction that, in the specific case characterized by a large number of tests, would produce a higher threshold. In addition, a visual identification will be also possible with the advantage that the elements identified and highlighted in the FE model arise from a rigorous statistical discriminatory procedure among investigated groups.

In the end of the present thesis a comparison between the critical elements belonging to FE model identified by the current methodology and those obtained analysing the whole area of neck and trochanter, conducted in a previous study without the support of RFT, is considered and discussed. Both analyses are performed considering the same sample of osteoporotic patients and FE results extracted by simulations. A second level of analysis and ROC curves will contribute to stand out the difference between the two different methods, in favour of the new statistical approach.

2 Materials and Method

2.1 Source of data

The methodology was applied to 111 patients (men and women), who have taken part in a previous study **[32]**. All subjects are osteoporotic patients: 62 patients had suffered of fracture located in the proximal femur (neck or trochanter) and 49 patients characterised by the lack of previous fracture. The use of clinical data, including DXA 2D images for the reconstruction of 3D FE model using the software 3D-Shaper®, were evaluated and approved by the ethics committee of the University Hospital Mutua de Terrassa **[32]**. A table with patient information about gender and type of fracture, for both recruited groups, is presented (Tab. 1).

The values, per elements, of Major Principal Stress (MPS) and Major Principal Strain (MPE) used for statistical analysis, are related to mechanical response of the bone to the event of the fall obtained from FE static simulations described in **[33]**. The unit of measurement of MPS and MPE are N/mm^2 (MPa) and mm/mm, respectively.

Gender	Fractures		Controls
	NECK	TROCHANTER	
Female patients	26	19	37
Male patients	10	07	12
Total patients	36	26	49

Table 1: Fractured and control patients

Briefly, the boundary conditions used for simulations concerning the application of fall force on the top of the femoral head and the constriction of the distal extremity of the femur. Also, the external surface of the greater trochanter in direction of the force was fixed (Fig. 11).

The force, applied to simulate the lateral fall is patient-specific and considerer the patient mass and weight according to the formula:

$$F_{fall}=\sqrt{2 \cdot g \cdot k_{tiss} \cdot m} \qquad [6]$$

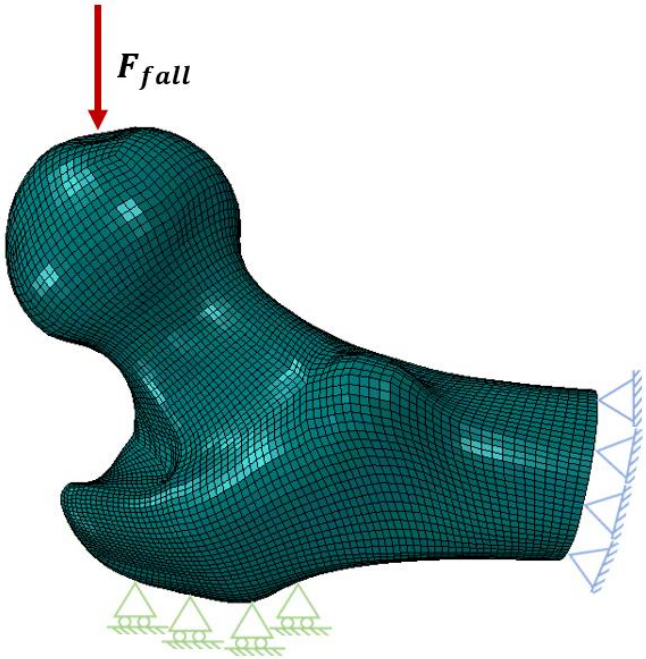

Figure 12: Boundary conditions applied to FE model

Where g is the gravity acceleration (9.81 m/s^2), k_{tiss} is a constant in relation to the stiffness of the trochanter soft tissue (71 N/mm), m is the mass of the specific patient and h_c the height of the centre of gravity related to the height h of the patient according to the formula:

$$h_c = 0.51 \cdot h \qquad [7]$$

The mass m is expressed in kilograms *kg* while h_c and h are in meters m.

In all FE patient specific femur models, for both groups (fractured and controls), two different types of tissue (trabecular and cortical) and different fracture areas (neck zone, trochanter zone, head zone and distal zone) are distinguishable (Fig. 12).

The femur tissues, cortical and trabecular, have a linear isotropic elastic behaviour. For cortical and trabecular bone, the Young' s modulus (E_{cort} and E_{trab}) in MPa is calculated by the following empirical expressions:

$$E_{cort} = 10200 \cdot \rho_{ash}^{2.01}, \text{ where } \rho_{ash} = 0.87 \cdot \rho_{QCT} - 0.079 \quad [8]$$

$$E_{trab} = 0.003715 \cdot \rho_{app}^{1.96}, \text{ where } \rho_{app} = \frac{\rho_{QCT}}{0.6} \quad [9]$$

In particular, ρ_{ash} and ρ_{QCT} represent the ash density of the bone and the radiological density (DXA for the current study), respectively. Both are expressed in g/cm^3. While ρ_{app} is the apparent density of the bone, in kg/m^3. Poisson's ratio is set at 0.3 for trabecular and cortical tissue.

Each patient specific model consists of the same number and type of elements (126,800 hexahedral elements) and same number of nodes (132,120). This means that all models have one-to-one correspondence, i.e. element 1 of model 1 is built by the same nodes that element 1 of model 2.

Such correspondence makes possible to consider a unique structural geometry as reference, where each element will correspond the value of a specific variable (MPS, MPE) for each osteoporotic patient.

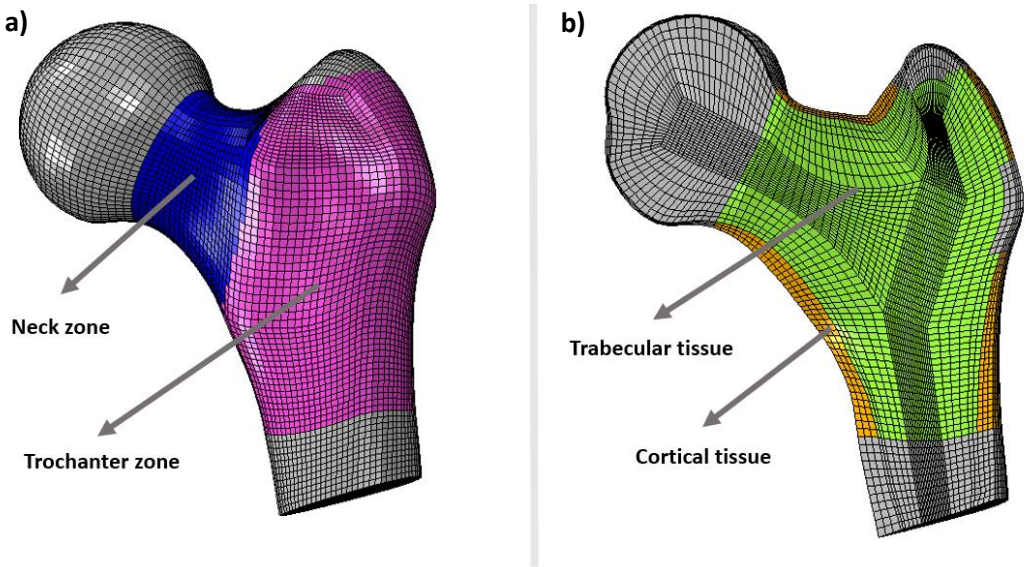

Figure 13:

a) Fracture zone: neck and trochanter *b) Bone tissue: trabecular and cortical*

Because the hip fracture, as is known by literature, usually occurs in the neck and trochanter area, the study started involving the elements belongs to these regions, shown in Fig. 13, with the purpose of reducing the critical regions. In addition, the elements on which the boundary conditions had been applied were removed. In this way, the impairment of average calculation is avoided. These modifications on the FE original geometry had led to a reduction of the number of elements and consequently of the number of nodes. Tab. 2 shows, for the new region of analysis, the number of elements and nodes in relation to the type of tissue.

Zone of analysis	Number of elements
Trabecular elements	68327
Cortical elements	16353
Total elements	84680

Table 2: Number of elements belonging to zone of analysis in relation to trabecular and cortical tissue

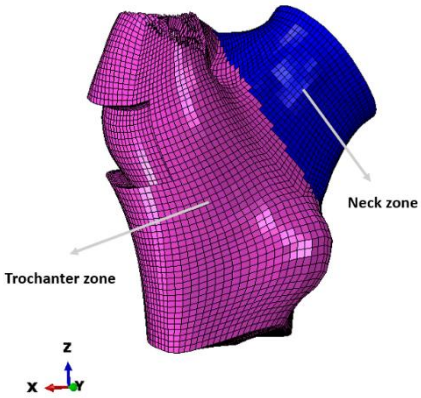

Figure 14: Zone of analysis

2.2 Design of experiment

The design of experiment of the thesis is organized in different steps and includes data organization that will be input data required for the use of statistical software named “spm1d”. The software allows to handle 1D experimental biomechanics data to compute statistical analysis (Two-sample t-test), which tests output are reported in a statistical parametric map (SPM).

The tests, implemented in MATLAB, that produce the rejection of null hypothesis will yield one or more statistically significant clusters identifying critical fracture regions visualized into FE model in Abaqus.

Successively, the significant elements of FE model detected by performing the Two-sample t-test, are implicated in the second level of analysis (Two-way ANOVA with repeated measures) to take into consideration the interaction between factors (group, fracture area, type of tissue) on the dependent variables (MPS, MPE).

In the end, to verify the reliability of this method of analysis, a comparison in relation to the ROC curves and to the area under the curves (AUC) was made considering the statistically significant elements belonging to the regions identified as critical and the more conservative analysis, that consider all elements of neck and trochanter was performed.

The figure below summarises the steps sequence implemented (Fig. 14).

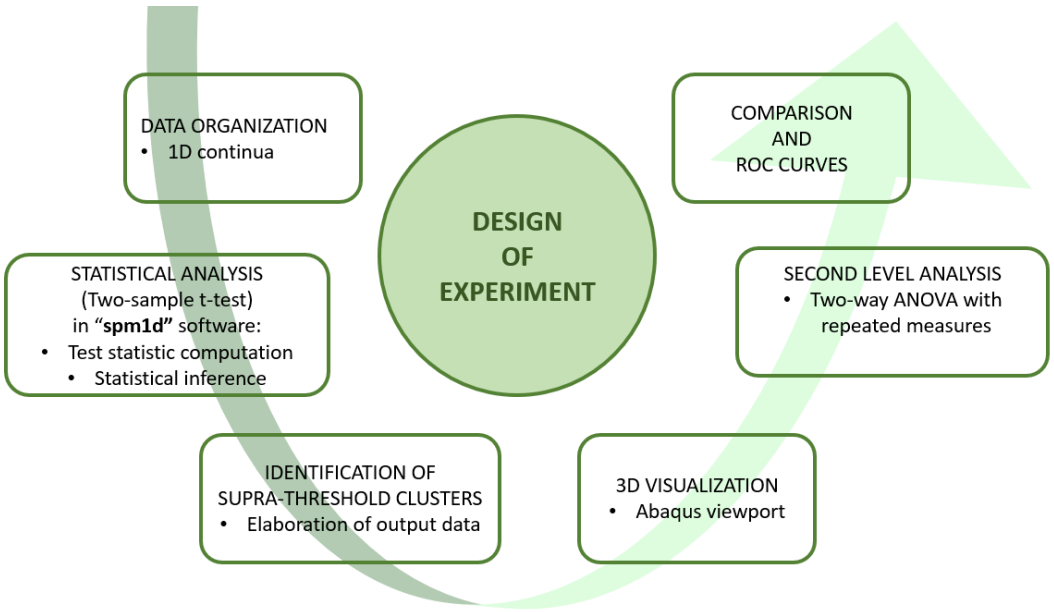

Figure 14: Design of experiment steps

2.2.1 Data organization

The results concerning MPS and MPE extracted by simulations represent the input data provided to software "spm1d" **[34]**. It is used to conduct statistical analysis between the two recruited groups (fractures and controls) in order to obtain one-dimensional statistical parametric maps (SPM).

The software, open source and implemented in MATLAB by Todd Pataky, requires experimental data described as "1D continua" (1D trajectories) to make statistical inferences under Random Field Theory (RFT) **[35]**. Therefore, come the need to organize data in a correct manner, starting from 3D geometry, according to a one-dimensional trajectory, thus allowing the use of the software.

A note concerning the choice of using the “spm1d” should be made.
Although the dataset originates from a three-dimensional geometry (FE femur model), and therefore the use of software able to process 3D data could be more appropriate, “spm1d” represent the only software, at the moment, that allow to handle data applying the RFT. Consequently, RFT makes possible to overcome the multiple comparison problem that occurs when a lot of dependent tests are performed, as in this instance.
For this reason, the great challenge of the present thesis is related to the way to treat spatial data according to an alternative and replaceable mono-dimensional perspective.

2.2.1.1 Creation of one-dimensional trajectory

The implementation of a one-dimensional field is obtained by replacing the 3D FE geometry with 1D ordered sequence of elements. Because each element belonging to the FE femur model consists of 8 nodes, only one node for each element has been chosen for the realization of the path. As a general criterion of choice, for each element the junction node corresponds to the node in the first position. In the even that different elements have the same junction node, an algorithm of choice (implemented in MATLAB) selects another reference node, among the potential 7 remaining, for the second repetitions. And so on for any subsequent repetitions. At the end of this procedure to each element, in which the variable of interest (MPS, MPE) is calculated, there is a corresponding node in the path. The list of nodes, nodes coordinates, elements, variables of interest were extracted from FE simulations, previously implemented in Abaqus.

To reduce the risk of spatial discontinuity the sequence of reference nodes in the path follows a logical order based on the minimum distance between them. The risk of discontinuity, due to different type of tissue, was indeed avoided achieving two distinct trajectories: one for trabecular tissue and one for cortical tissue.

The algorithm, known the spatial coordinate of each reference node, proceeds in steps:

1. Arbitrary choice of the first node of the path. It represents the origin of the one-dimensional trajectory.

2. Calculation of Euclidean distance between the origin node of the path and all reference nodes. The node with the minimum distance from the origin will be the second node of the trajectory.
3. Calculation of Euclidean distance between the second node in the path and all remaining reference nodes. The node with the minimum distance from the second node will be the third node in the trajectory.
4. The algorithm is repeated until the path containing all reference nodes is created.
5. Adding up all the distances between a reference node and its previous in the path, the total distance from the origin is obtained (Fig. 15).

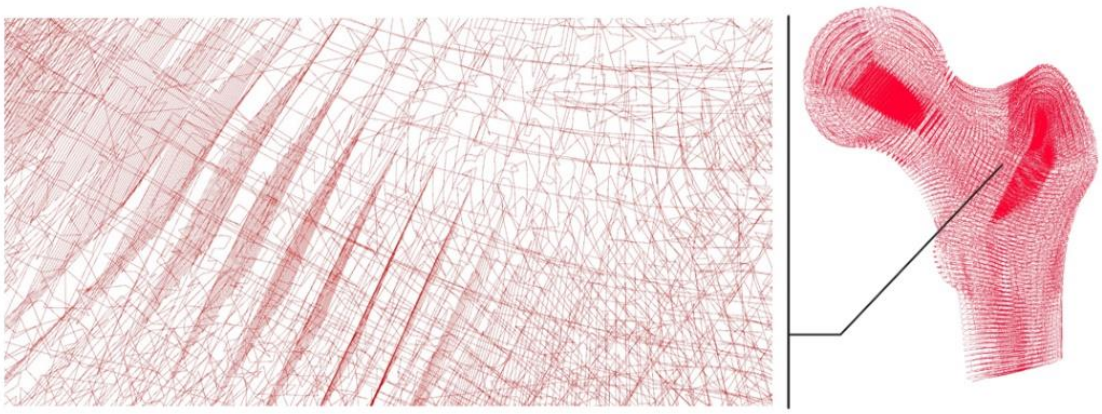

Figure 15: 1D trajectory of the FE femur model

At the end of the 5th steps, each patient for each investigated group will be represented by a one-dimensional ordered sequence of elements of FE model, identified by reference node, for which is known the variable of interest as result of FE simulations. It is important to remember that the ordered sequence of elements is the same for each patient because each patient-specific FE model consists of the same mesh with the same type and number of elements, same number of nodes with one-to-one correspondence. What changes between patients is the value of maximum absolute stress and maximum absolute strain associated with each element of the trajectory.

The flow chart of the algorithm previously described is presented (Fig. 16):

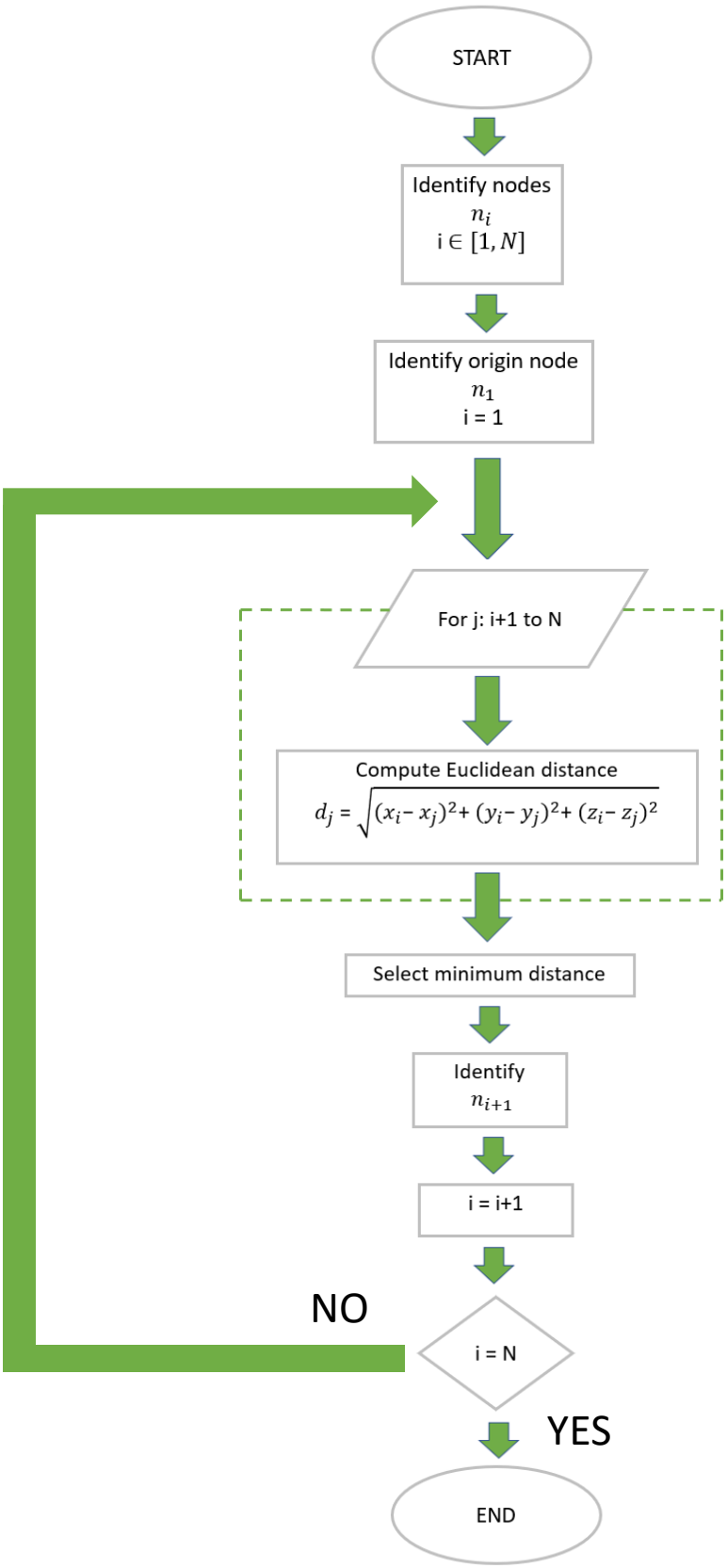

Figure 16: Flow chart of the algorithm

Fig. 17 shows, in relation to the zone of analysis (neck and trochanter area), the trajectory consisting of only trabecular reference nodes, the trajectory consisting of only cortical reference nodes and the trajectory that include trabecular reference nodes follow cortical reference nodes.

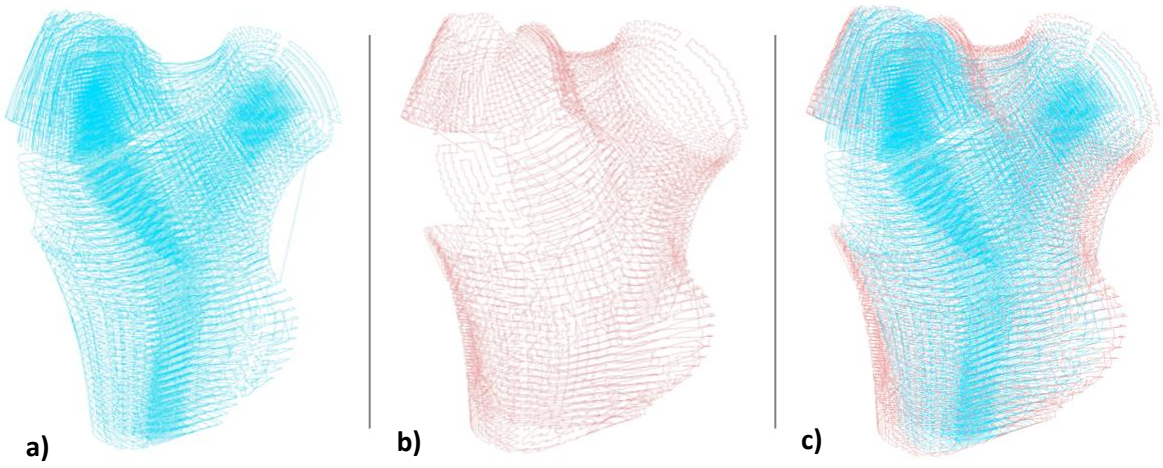

Figure 17:

a) 1D trajectory of trabecular tissue *b) 1D trajectory of cortical tissue* *c) 1D trajectory of both tissues: trabecular and cortical*

Although the algorithm was implemented in MATLAB, a better visualization of 1D trajectory was realized by importing the sequence of reference node coordinates, according to the logical order obtained by algorithm, in “Grasshopper 3D” that runs within the “Rhinoceros 3D” application.

2.2.1.2 Input data

“spm1d” requires experimental dataset, for both group (fractures and controls), arranged as a (J x Q) array, where:

- $\mathbf{J}$ - number of 1D responses. The number of responses corresponds to the number of subjects/patients for each recruited group.
- $\mathbf{Q_t}$ - number of points, identified by trajectory elements belonging to trabecular tissue, in the 1D continuum.
- $\mathbf{Q_c}$ - number of points, identified by trajectory elements belonging to cortical tissue, in the 1D continuum.

2.2.2 Statistical Parametric Map

The Statistical Parametric Map (SPM) is defined as the construction of spatially extended statistical processes to test hypotheses about regionally specific effects **[36]**. SPMs report the results of statistical analysis assembled in a statistic continuum SPM{t}, whose parameters are distributed according to the probability density function (Student's *t* distribution) by referring to the probabilistic behaviour of Gaussian field **[35] [17] [37] [38]**.

The test outputs of SPM include:

- **SPM.z** – 1D test statistic field during the path along continuum points of trabecular and cortical tissue.
- **SPM.df** – degrees of freedom.
- **SPM.FWHM** – The estimated full-width at half maximum of 1D Gaussian Kernel which produces the same smoothness of observed residuals in the case of it is convolved with 1D Gaussian continua.
- **SPM.resels** – Resolution elements that represent the total number of independent processes in the continuum. The formula is:

  Q = number of continuum points.
  EC = Euler characteristic, defined as the number of "holes" in the continuum.

  $$Resels = \frac{(Q - EC)}{FWHM} \qquad [10]$$

- **SPM.alpha** – Error type I, set at specific alpha value, identified by user.
- **SPM.z_star** – Critical Random Field Theory threshold.
- **SPM.H_0** – It may assume two different values. If test statistic continuum exceeds z_star, H_0 is equal to 1 and it means that the null hypothesis is rejected. Otherwise H_0 is equal to 0 and in this case the null hypothesis is accepted. It means there is no difference between the investigated group.
- **SPM.p** – It defines how many supra-threshold clusters have been generated. It is possible to access to each cluster's probability value.

2.2.3 Statistical analysis of 1D continua: Two-sample t-test

Two-sample (independent) t-tests, performed using “spm1d”, were applied to examine the effects of MPS and MPE in fractures and controls groups, taking into consideration gender (male and female), type of tissue (trabecular and cortical) and the region of fracture (neck or trochanter). Tab. 3 and Tab. 4 with all tests performed, on MPS and MPE variables, ere presented.

Variable	Two sample t-test		Group 1	Group 2
MPS	1		Fracture_neck_female	Control_female
		1.a	TRABECULAR	
		1.b	CORTICAL	
	2		Fracture_neck_male	Control_male
		2.a	TRABECULAR	
		2.b	CORTICAL	
	3		Fracture_trochanter_female	Control_female
		3.a	TRABECULAR	
		3.b	CORTICAL	
	4		Fracture_trochanter_male	Control_male
		4.a	TRABECULAR	
		4.b	CORTICAL	

Table 3: Two-sample t-test conducted on MPS variable

Variable	Two sample t-test		Group 1	Group 2
MPE	5		Fracture_neck_female	Control_female
		5.a	TRABECULAR	
		5.b	CORTICAL	
	6		Fracture_neck_male	Control_male
		6.a	TRABECULAR	
		6.b	CORTICAL	
	7		Fracture_trochanter_female	Control_female
		7.a	TRABECULAR	
		7.b	CORTICAL	
	8		Fracture_trochanter_male	Control_male
		8.a	TRABECULAR	
		8.b	CORTICAL	

Table 4: Two-sample t-test conducted on MPE variable

For 1D dataset, the goal is to quantify the probability that smooth, random 1D continua would produce a test statistic continuum whose maximum exceeds a particular test statistic value **[39]**.

Before conducting tests, the 1D continuum, for each patient, is smoothed using the full width of half-maximum (FWHM) of a Gaussian kernel arbitrarily selected equal to 25, which corresponds approximately to 2 cm. The spatial smoothness essentially increases the signal to noise ratio, reduce influence of functional, anatomical and physiological difference between subject improving the probability of identify commonalities between them. It also allows to use the RFT for thresholding passing through the calculation of standardized residuals from the general linear model (GLM).

In “spm1d” statistical testing is conducted in stages:

1. **Test statistic continuum computation** – Two-sample t-test. The tests take into account the spatial correlation applying the RFT.

2. **Statistical inference** – Two tailed inference at alpha specified. Alpha value identifies the probability to reject the null hypothesis when the hypothesis is true. Because two are the variables of interest, alpha value is set to alpha=0.05/2=0.025 (Bonferroni correction).

```
%% SPM{t}

%TEST STATISTIC COMPUTATION
spm_t2m=spm1d.stats.ttest2(Group_1,Group_2);

%STATISTICAL INFERENCE
spmi_t2m= spm_t2m.inference(0.025,'two_tailed',true);
disp(spmi_t2m);
```

Test statistic computation and statistical inference code lines

Where SPM{t} is above the critical RFT threshold, one or more clusters of elements are identified as significant. Each cluster is defined by a specific p-value, equal or less than alpha, for which the null hypothesis is rejected. It means that there is statistical difference between the examined groups, related to the dependent variable (MPS, MPE), associated with specific spatial regions of FE femur model. Otherwise, if the 1D test statistic field SPM{t} doesn’t reach the critical threshold, no supra-threshold clusters will be generated, and the null hypothesis will not be rejected.

2.2.4 Supra-threshold clusters

Test output, obtained by SPM, provides the first and last index belonging to each supra-threshold cluster along the 1D elements trajectory.

The indexes are achieved in decimal terms. So, the first acquired index must be truncated to the integer value plus one, while the last index has to be just truncated to the integer value. In this way the indexes obtained will concern only elements embedded in the supra-threshold clusters (Fig. 18).

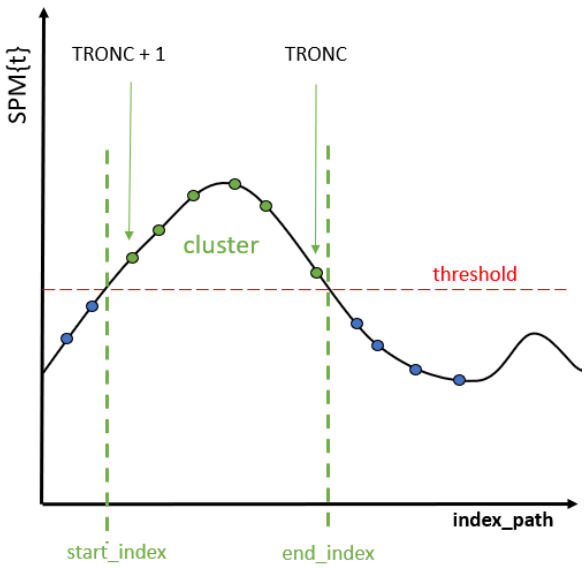

Figure 18: Statistically significant elements belonging to supra-threshold cluster

Associating the start and the end element corresponding to the indexes achieved and including the interposed elements, the trabecular and cortical vector of statistically significant elements are obtained. Because the test statistic computation in relation to type of tissue is separate, it is necessary to add the total number of trabecular elements to the indexes provided for cortical tissue. It is because the original 1D trajectory includes cortical elements that follow the trabecular elements. Index vector is used not only to extract the statistically significant elements in that specific position along the 1D trajectory, but also to associate the corresponding absolute maximum stress and absolute maximum strain with them. So, for each patient a vector containing the values of dependent variable (MPS/MPE) along the 1D continuum is created, from which the main value and standard deviation may be computed. To be exact, to each subject corresponds a mean value and standard deviation in relation to the dependent variable both for trabecular and cortical tissue.

2.2.5 3D visualization in FE model

Once defined the elements belonging to each supra-threshold cluster obtained from Two-sample t-test computed into “spm1d”, just import them into a file text that uses comma to separate elements (.CSV) and then into the FE solver Abaqus (Dassault Systèmes) viewport of the FE model for a 3D visualization of critical hip fracture regions identified in the previous sub-section.

2.2.6 Second level analysis: Two-way ANOVA with repeated measures

Another type of statistical analysis computed is the Two-way ANOVA with repeated measures with the purpose of establishing if there is a statistically significant interaction between factors on the dependent variable. The two factors (“Group” and “Type of tissue”) represent the independent variables, also defined as “between subjects’ factor” and “within subjects’ factor” respectively.

Using the mean value and standard deviation of MPS/MPE, the univariate analysis involves individual variables in the dataset to better understand its distribution of values.

Gender	Dependent variable	Group 1	Group 2
Female	Stress_mean Stress_std	Control	FractNeck
		TRABECULAR	
		CORTICAL	

Gender	Dependent variable	Group 1	Group 2
Female	Stress_mean Stress_std	Control	FractTroc
		TRABECULAR	
		CORTICAL	

Gender	Dependent variable	Group 1	Group 2
Female	Strain_mean Strain_std	Control	FractTroc
		CORTICAL	

Table 5: Comparisons among groups computed in second level analysis.

In this second level of analysis only the comparisons that produced supra-threshold clusters have been considered (Tab. 5).

Tested groups include only female osteoporotic patients. This is because the number of male patients is not enough for a consistent analysis.

Although Two-way ANOVA with repeated measures has not been performed into “spm1d” because of unbalanced groups (26 Fracture_neck_female/ 37 Control_female; 19 Fracture_trochanter_female/ 37 Control_female), it was nevertheless computed for its complementary role to the statistical analysis previously conducted (Two-sample t-test).

2.2.7 Comparison and ROC curves

The results of the second level analysis derived by the identification of the statistically significant areas identified using SPM, were finally compared to the analysis performed over the whole neck and trochanteric regions (Fig. 19). The capability of discriminate fracture from control subjects was tested performing a ROC analysis and computing the area under the curve (AUC) for the parameters identified.

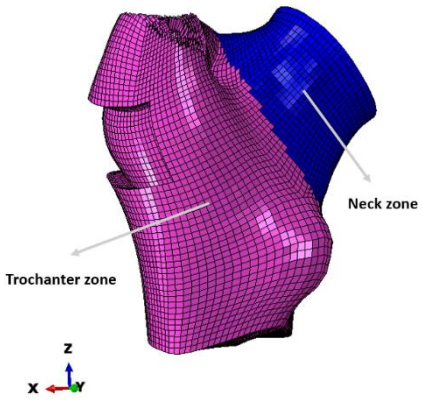

Figure 19: Zone of analysis

The input features were all the significant variables identified in the second level analysis plus possible significant interactions. Variables representing significant interactions were computed making the difference between the value computed in the two levels of the within factor and comparing the results between fracture and control subjects. The final classification was evaluated by comparing the resulting confusion matrices, which provide us how many patients are classified in the control group and in the fractured group.

In the end the variables extracted from the two different analyses, considering the elements belonging to the whole area of neck and trochanter and only statistically significant elements identified in this present thesis respectively, were used to plot the ROC curves (Receiver Operating Characteristic). A comparison between the ROC curves of the two analyses was performed to demonstrate advantages and improvements brought by the new approach.

The purpose of using the ROC curve is essentially to evaluate the diagnostic power of the methodology adopted through an accuracy measure in relation to sensibility and specificity.

3 Results

3.1 Two-sample t-test

The results of the analysis are shown in SPMs (Fig. 20-21). For each comparison reported in Tab. 3 and in Tab. 4 have been obtained different SPMs in relation to the different variable of interest (MPS/MPE), type of tissue (trabecular/cortical), gender (male/female) and type of fracture (neck/trochanter). The graphs show the variation of the dependent variable along the order sequence of elements in the path. The thick black line depicts the test statistic continuum SPM{t}, while the red dashed line the critical threshold t^* at α value.

- **Major Principal Stress variable**

a)

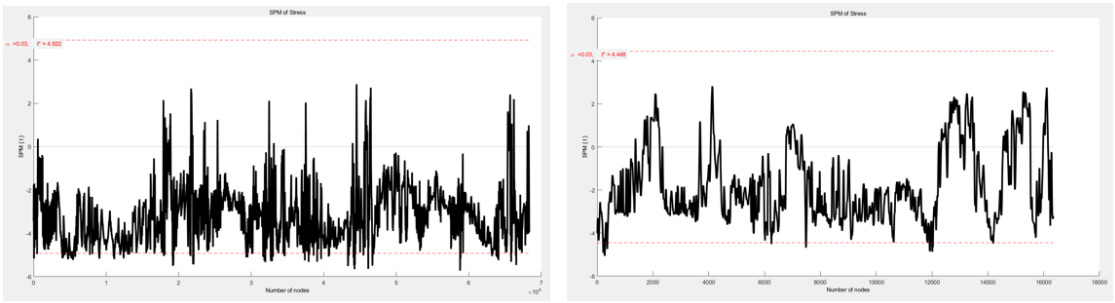

Figure 20:

a)SPMs obtained by Two-sample t-test between Neck_fracture_female and Control_female on the variable MPS in relation to trabecular (on the left) and cortical (on the right) tissue. Both tests continuum SPM{t} exceed the threshold.

b)

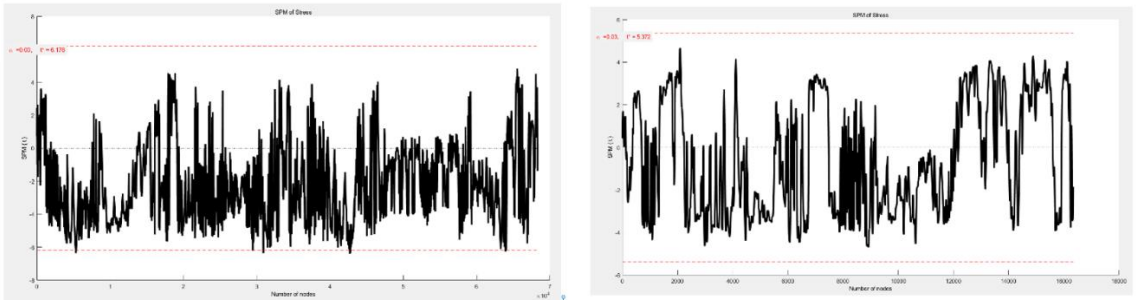

Figure 20:

b)SPMs obtained by Two-sample t-test between Neck_fracture_male and Control_male on the variable MPS in relation to trabecular (on the left) and cortical (on the right) tissue. Only test continuum SPM{t} concerning trabecular tissue exceeds the threshold.

c)

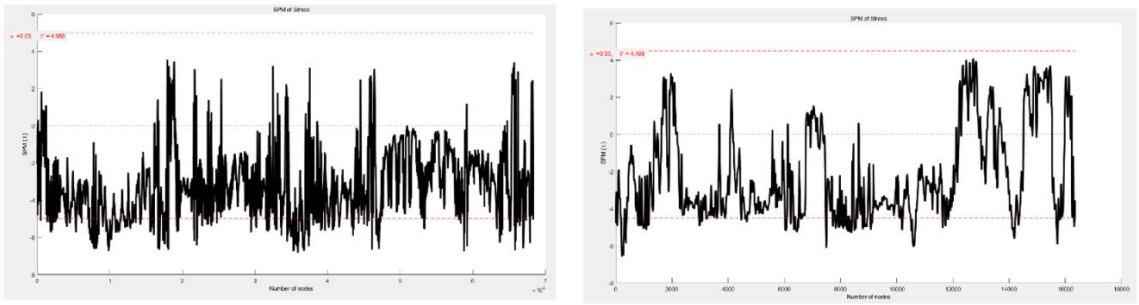

Figure 20:

c)SPMs obtained by Two-sample t-test between Trochanter_fracture_female and Control_female on the variable MPS in relation to trabecular (on the left) and cortical (on the right) tissue. Both tests continuum SPM{t} exceed the threshold.

d)

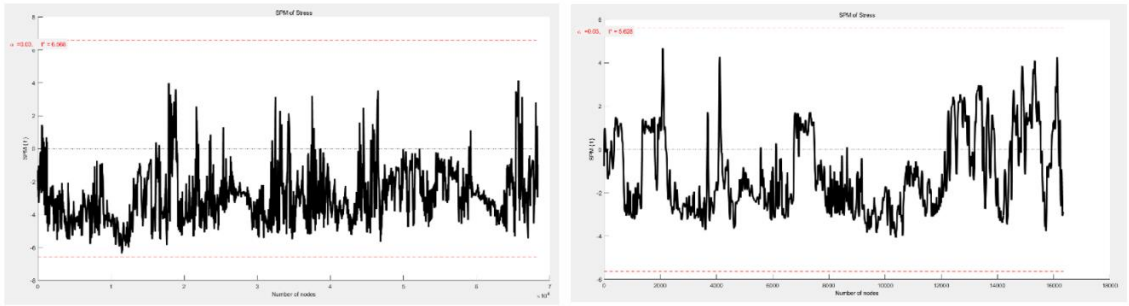

Figure 20:

d)SPMs obtained by Two-sample t-test between Trochanter_fracture_male and Control_male on the variable MPS in relation to trabecular (on the left) and cortical (on the right) tissue. Neither of tests continuum SPM{t} exceed the threshold.

- **Major Principal Strain variable**

a)

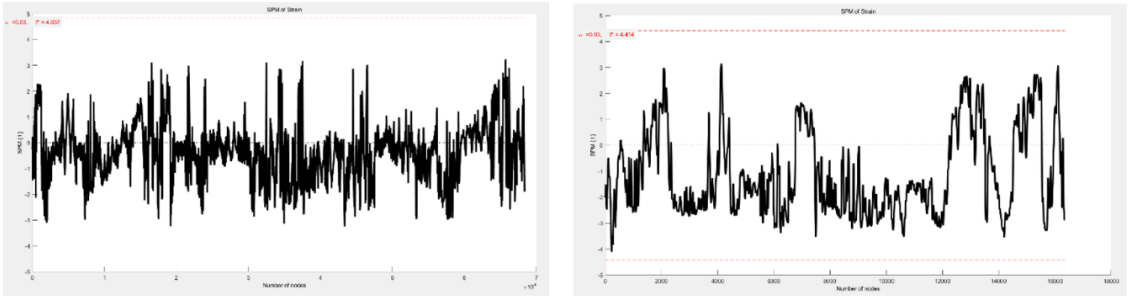

Figure 21:

a)SPMs obtained by Two-sample t-test between Neck_fracture_female and Control_female on the variable MPE in relation to trabecular (on the left) and cortical (on the right) tissue. Neither of tests continuum SPM{t} exceed the threshold.

b)

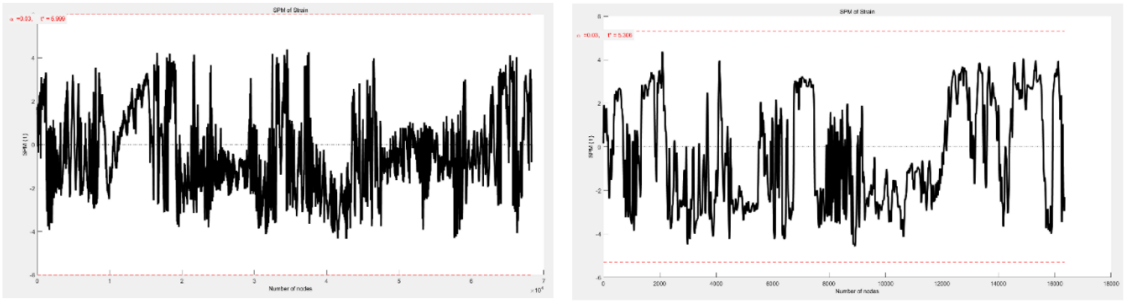

Figure 21:

b)SPMs obtained by Two-sample t-test between Neck_fracture_male and Control_male on the variable MPE in relation to trabecular (on the left) and cortical (on the right) tissue. Neither of tests continuum SPM{t} exceed the threshold.

c)

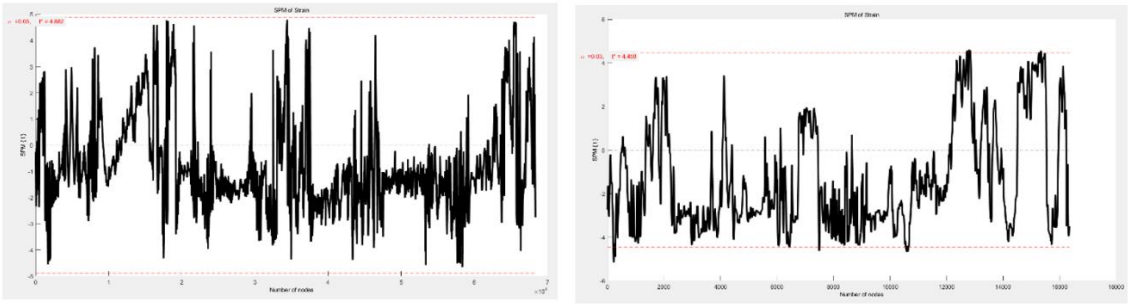

Figure 21:

c)SPMs obtained by Two-sample t-test between Trochanter_fracture_female and Control_female on the variable MPE in relation to trabecular (on the left) and cortical (on the right) tissue. Only test continuum SPM{t} concerning cortical tissue exceeds the threshold.

d)

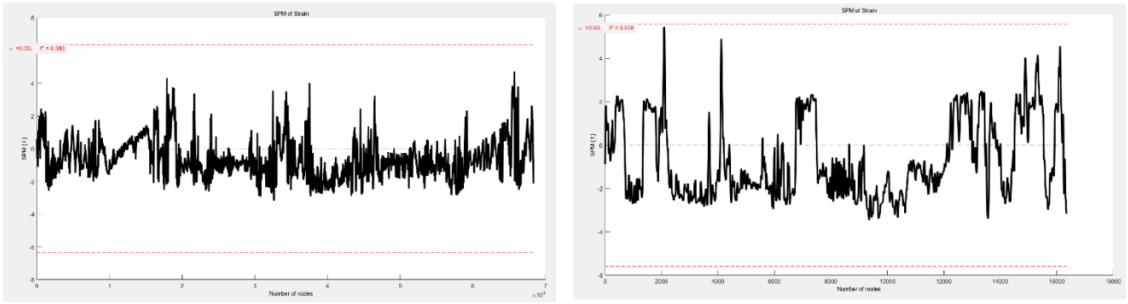

Figure 21:

d)SPMs obtained by Two-sample t-test between Trochanter_fracture_male and Control_male on the variable MPE in relation to trabecular (on the left) and cortical (on the right) tissue. Neither of tests continuum SPM{t} exceed the threshold.

Test outputs of each SPM, in relation to test statistic computation and statistical inference, are reported in Tab. 6 and Tab. 7. The cells highlighted identify the tests in which the null hypothesis is not rejected.

Variable	SPM{t} inference	Fracture_neck_female-Control_female		Fracture_neck_male-Control_male		Fracture_trochanter_female-Control_female		Fracture_trochanter_male-Control_male	
		TRABECULAR	CORTICAL	TRABECULAR	CORTICAL	TRABECULAR	CORTICAL	TRABECULAR	CORTICAL
MPS	z	[1x68327]	[1x16353]	[1x68327]	[1x16353]	[1x68327]	[1x16353]	[1x68327]	[1x16353]
	df	[1 61]	[1 61]	[1 20]	[1 20]	[1 54]	[1 54]	[1 17]	[1 17]
	FWHM	63.2968	75.4238	56.6887	71.2782	62.6662	74.8205	58.7313	76.4087
	Resels	[1 1.0795e+03]	[1 216.8016]	[1 1.2053e+03]	[1 229.4108]	[1 1.0903e+03]	[1 218.5496]	[1 1.1634e+03]	[1 214.0072]
	alpha	0.0250	0.0250	0.0250	0.0250	0.0250	0.0250	0.0250	0.0250
	z_star	4.9218	4.4482	6.1781	5.3716	4.9881	4.4991	6.5677	5.6277
	H_0_reject	1	1	1	0	1	1	0	0
	p_set	0	0	0	1	0	0	1	1
	p	[1x81]	[1x9]	[1x7]	[]	[1x173]	[1x54]	[]	[]

Table 6: SPM{t} statistical inference on variable MPS in relation to compared groups (fractured/controls), zone of fracture (neck/trochanter), type of tissue (trabecular/cortical) and gender (female/male).

Variable	SPM{t} inference	Fracture_neck_female-Control_female		Fracture_neck_male-Control_male		Fracture_trochanter_female-Control_female		Fracture_trochanter_male-Control_male	
		TRABECULAR	CORTICAL	TRABECULAR	CORTICAL	TRABECULAR	CORTICAL	TRABECULAR	CORTICAL
MPE	z	[1x68327]	[1x16353]	[1x68327]	[1x16353]	[1x68327]	[1x16353]	[1x68327]	[1x16353]
	df	[1 61]	[1 61]	[1 20]	[1 20]	[1 54]	[1 54]	[1 17]	[1 17]
	FWHM	84.8308	84.5453	81.4896	81.7322	89.3105	85.3979	87.2884	83.8168
	Resels	[1 805.4388]	[1 193.4110]	[1 838.4632]	[1 200.0681]	[1 765.0385]	[1 191.4801]	[1 782.7619]	[1 195.0922]
	alpha	0.0250	0.0250	0.0250	0.0250	0.0250	0.0250	0.0250	0.0250
	z_star	4.8370	4.4137	5.9991	5.3062	4.8820	4.4579	6.3427	5.5778
	H_0_reject	0	0	0	0	0	1	0	0
	p_set	1	1	1	1	1	0	1	1
	p	[]	[]	[]	[]	[]	[1x10]	[]	[]

Table 7: SPM{t} statistical inference on variable MPE in relation to compared groups (fractured/controls), zone of fracture (neck/trochanter), type of tissue (trabecular/cortical) and gender (female/male).

The tests, concerning the variable MPS, produce supra-threshold clusters except in the comparison between Fracture_neck male/Control_male in relation of cortical tissue and between Fracture_trochanter_male/Control_male in both tissues.

By contrast, the tests concerning the variable MPE, do not produce any supra-threshold clusters except in the comparison between Fracture_trochanter_female/Control_female in relation to cortical tissue.

In the Tab. 8 and Tab.9, are indeed reported, for each Two-sample t-test concerning MPS and MPE, the number and the percentage of significant statistical elements compared to the total and belonging to trabecular and cortical tissue, respectively.

a)

Variable	TWO SAMPLE T2TEST	TRABECULAR ELEMENTS	CORTICAL ELEMENTS	TOTAL ELEMENTS
MPS	Fracture_neck_female-Control_female	2350	171	2521
	Fracture_neck_male-Control_male	133	0	133
	Fracture_trochanter_female-Control_female	11180	2333	13513
	Fracture_trochanter_male-Control_male	0	0	0

Table 8 (a: Number of statistically significant elements, concerning variable MPS, belonging to trabecular and cortical tissue and both.

b)

Variable	TWO SAMPLE T2TEST	TRABECULAR ELEMENTS (%)	CORTICAL ELEMENTS (%)	TOTAL ELEMENTS (%)
MPS	Fracture_neck_female-Control_female	3.44 %	1.04 %	2.97 %
	Fracture_neck_male-Control_male	0.19 %	0	0.16 %
	Fracture_trochanter_female-Control_female	16.36 %	14.26 %	15.96 %
	Fracture_trochanter_male-Control_male	0	0	0

Table 8 (b: Number of statistically significant elements (in terms of percentage) concerning the variable MPS, belonging to trabecular and cortical tissue. Also the percentage compared to the total is reported.

a)

Variable	TWO SAMPLE T2TEST	TRABECULAR ELEMENTS	CORTICAL ELEMENTS	TOTAL ELEMENTS
MPE	Fracture_neck_female-Control_female	0	0	0
	Fracture_neck_male-Control_male	0	0	0
	Fracture_trochanter_female-Control_female	0	260	260
	Fracture_trochanter_male-Control_male	0	0	0

Table 9 (a: Number of statistically significant elements, concerning variable MPE, belonging to trabecular and cortical tissue and both.

b)

Variable	TWO SAMPLE T2TEST	TRABECULAR ELEMENTS (%)	CORTICAL ELEMENTS (%)	TOTAL ELEMENTS (%)
M P E	Fracture_neck_female-Control_female	0	0	0
	Fracture_neck_male-Control_male	0	0	0
	Fracture_trochanter_female-Control_female	0	1.59 %	0.30 %
	Fracture_trochanter_male-Control_male	0	0	0

Table 9 (b: Number of statistically significant elements (in terms of percentage) concerning the variable MPE, belonging to trabecular and cortical tissue. Also the percentage compared to the total is reported.

3.1.2 3D visualization in FE model

The 3D visualization, reported in Fig. 22, provides statistically significant elements belonging to trabecular tissue, cortical tissue and both tissues, respectively. Only the 3D visualizations of the proximal femur result from tests that have produced supra-threshold clusters are shown. Significant elements are marked in red.

a)

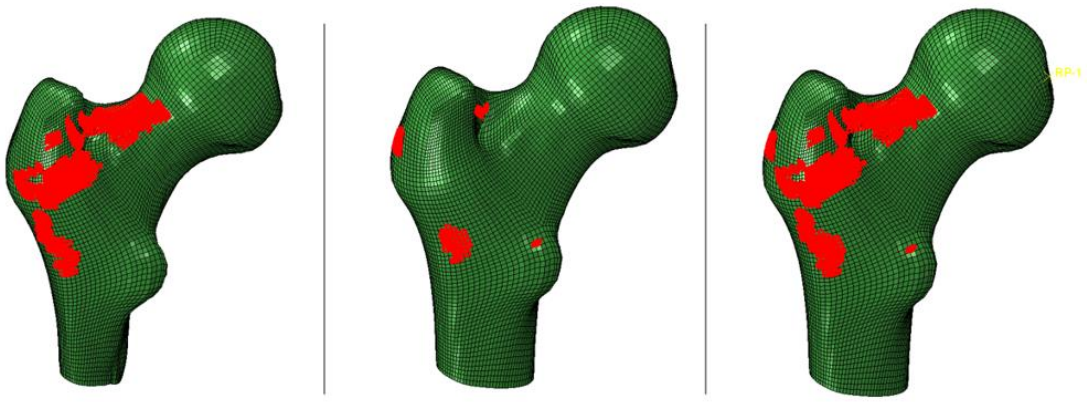

Figure 22:

a)3D visualization of statistically significant elements obtained by Two-sample t-test between Neck_fracture_female and Control_female concerning the variable MPS in relation to trabecular tissue, cortical tissue and both tissues respectively. There are significant elements belonging both trabecular and cortical tissue.

b)

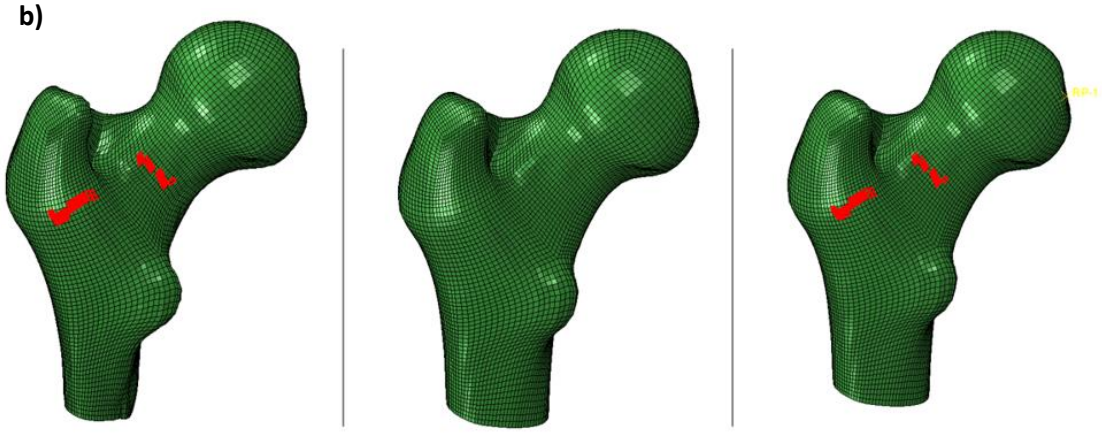

Figure 22:

b)3D visualization of statistically significant elements obtained by Two-sample t-test between Neck_fracture_male and Control_male concerning the variable MPS in relation to trabecular tissue, cortical tissue and both tissues respectively. There are significant elements only in trabecular tissue.

c)

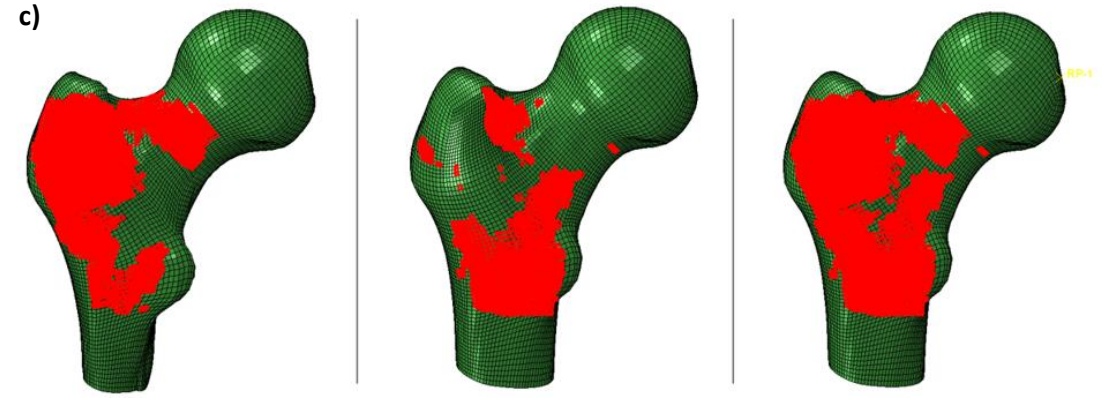

Figure 22:

c)3D visualization of statistically significant elements obtained by Two-sample t-test between Trochanter_fracture_female and Control_female concerning the variable MPS in relation to trabecular tissue, cortical tissue and both tissues respectively. There are significant elements belonging both trabecular and cortical tissue.

d)

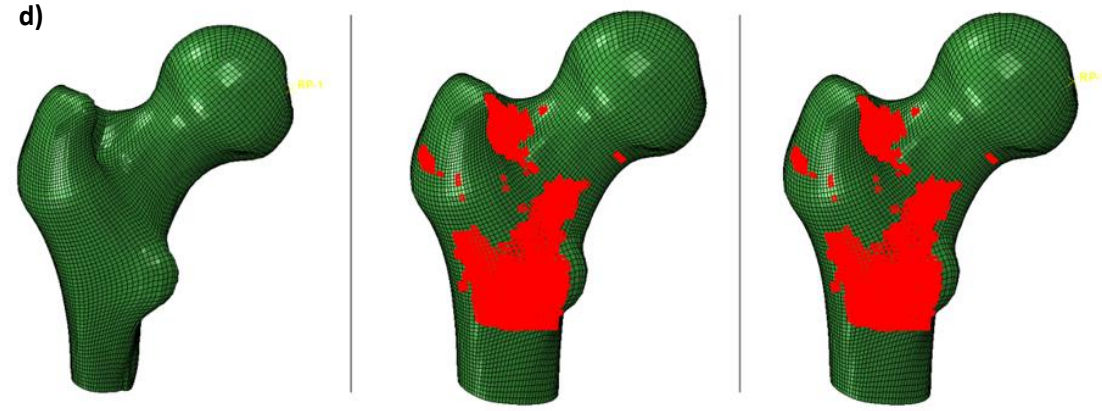

Figure 22:

d)3D visualization of statistically significant elements obtained by Two-sample t-test between Trochanter_fracture_female and Control_female concerning the variable MPE in relation to trabecular tissue, cortical tissue and both tissues respectively. There are significant elements only in cortical tissue.

3.2 Mean and Standard Deviation

For each comparison reported in Tab. 3 and Tab. 4, the tables shown in Appendix I provide, for each patient belonging to each tested group, the mean value and standard deviation calculated in relation to the dependent variables associated to the elements that exceed the threshold. As noted above, the tests concerning the variable MPS produce statistically significant elements in each comparison except between Fracture_neck_male/Control_male on cortical tissue and between Fracture_trochanter_male/Control_male patients. The variable MPE produces clusters only comparing Fracture_trochanter_female and Control_female patients. In this test the results can be divided for each group in two tables: one about the mean and std for each patient calculated from the elements that exceed the threshold below the z_critic and the other one about the mean and std for each patient derived from the elements that exceed the threshold above the z_critic.

3.3 Two-way ANOVA with repeated measures

To explore deeper the interaction between the levels of the independent factors on the dependent variable, the estimated marginal means obtained by multifactorial ANOVA have been considered and graphed.

The estimated marginal means is more appropriate than the means to detect the interaction in a correct manner because it reflects the mean response for each factor, adjusted for any other variables in the model.

Only the variables identified as significant in the SPM analysis were tested using the Two-way ANOVA.

In this second level analysis male gender has been excluded because of the reduced number of patients. The bar charts (Fig. 23-24-25), for each comparison that exceeds the threshold of the Two-sample t-test, report the estimated mean and the standard error in relation to the mean and std of the dependent variable (Stress_mean, Stress_std, Strain_mean, Strain_std) taking into consideration the two factors (1. Group, 2. Tissue / 1. Group, 2. Reduced_Increased) separately and the interaction between them (3. Group*Tissue /3. Group*Reduced_Increased).

In particular, three univariate analyses have been performed.

The first and second univariate analysis concern the dependent variable MPS (Stress_mean, Stress_std) while the independent variables are represented by the investigated groups (Control/FractNeck and Control/FractTroc, respectively) and the type of tissue (trabecular and cortical in both cases). The group is the “between subjects’ factor” while the tissue the “within subjects’ factor”.

In the last multivariate analysis the dependent variable is represented by MPE (Strain_mean, Strain_std) while the first independent variable (”between subjects factor”) is defined by the investigated groups (Control/FractTroc) in relation to cortical tissue. The second dependent variable (“within subjects”) concerns the value of MPE that exceeded the threshold below and above identifying regions in which the variable strain increases and decreases respectively in cortical tissue of fractured subject compared to the one of the controls (Reduced_Increased label). Trabecular tissue is not taken into consideration because, for the independent variable MPE, there are not significant elements detected. Also in this analysis only female patients have been considered.

In addition, the ANOVA multifactorial results are graphed (Fig. 23(d-24(d-25(d)) considering the estimated marginal means of the interaction between factors on the mean and std of the dependent variable (Stress_mean, Stress_std, Strain_mean, Strain_std).

- **Neck Analysis on mean value and std of MPS**

a)

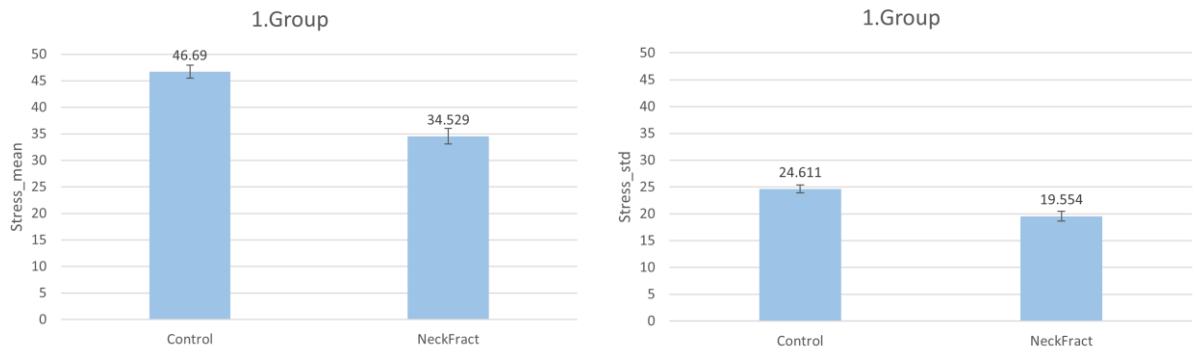

Figure 23:

a)Neck analysis on mean value and std of MPS. Estimated mean and std.Error are graphed in relation to the first factor identified by “Group” (Control-NeckFract).

b)

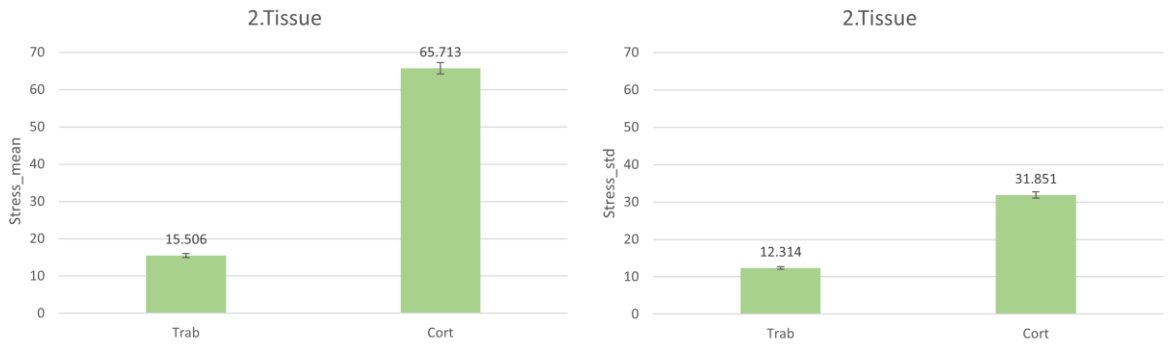

Figure 23:

b)Neck analysis on mean value and std of MPS. Estimated mean and std.Error are graphed in relation to the second factor identified by "Tissue" (Trab-Cort).

c)

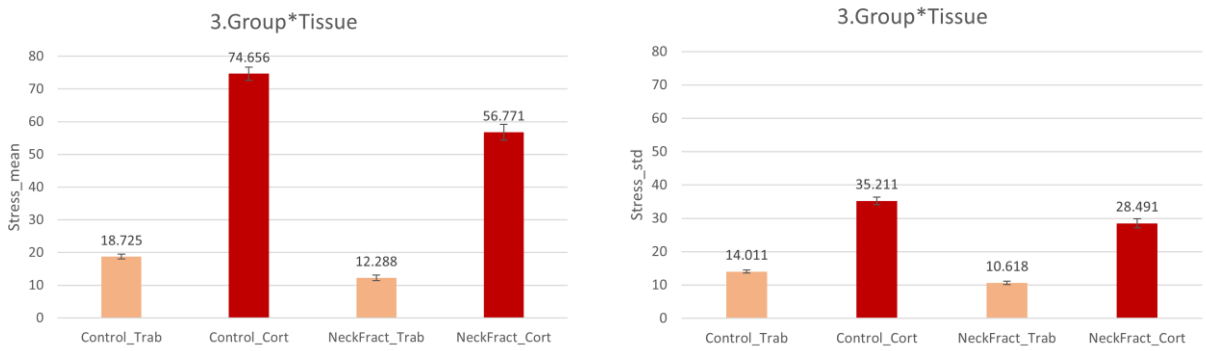

Figure 23:

*c)Neck analysis on mean value and std of MPS. Estimated mean and std.Error are graphed in relation to the interaction between factors identified by "Group*Tissue".*

d)

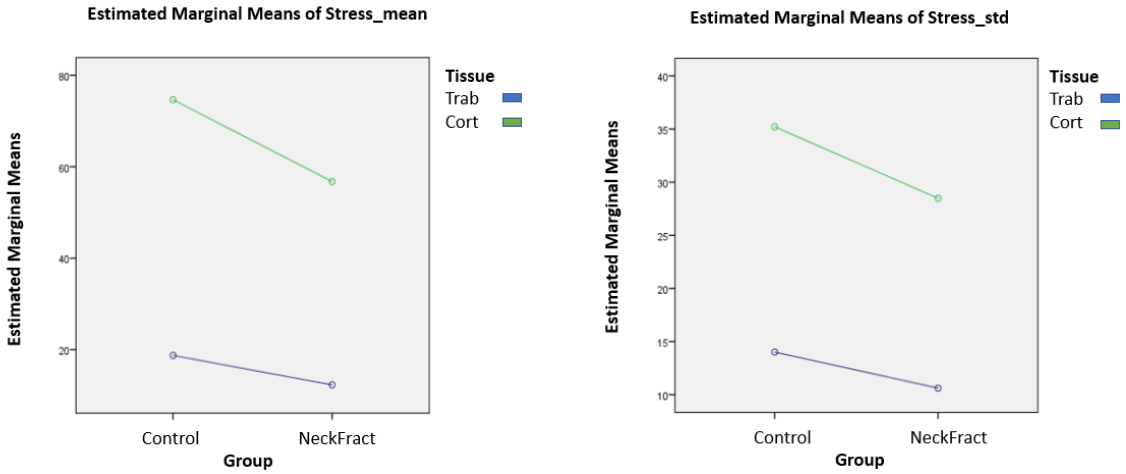

Figure 23:

*d)Neck analysis on mean value and std of MPS. Estimated marginal means are graphed in relation to the interaction between factors identified by "Group*Tissue".*

NeckAnalysis				
Stress				
	1. Group	2. Tissue	mean	Std.Error
Stress_mean	Control	Trab	18.725	0.718
		Cort	74.656	1.994
	NeckFract	Trab	12.288	0.857
		Cort	56.771	2.379
Stress_std	Control	Trab	14.011	0.437
		Cort	35.211	1.092
	NeckFract	Trab	10.618	0.522
		Cort	28.491	1.302

Table 10: Neck analysis on mean value and std of MPS.

*Estimated marginal means are reported in relation to the interaction between factors identified by "Group*Tissue".*

- **Trochanter Analysis on mean value and std of MPS**

a)

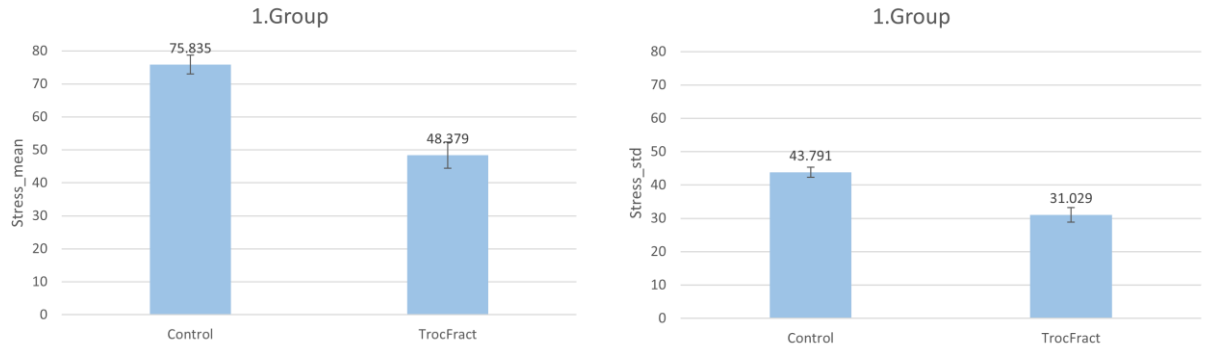

Figure 24:

a)Trochanter analysis on mean value and std of MPS. Estimated mean and std.Error are graphed in relation to the first factor identified by "Group" (Control-TrocFract).

b)

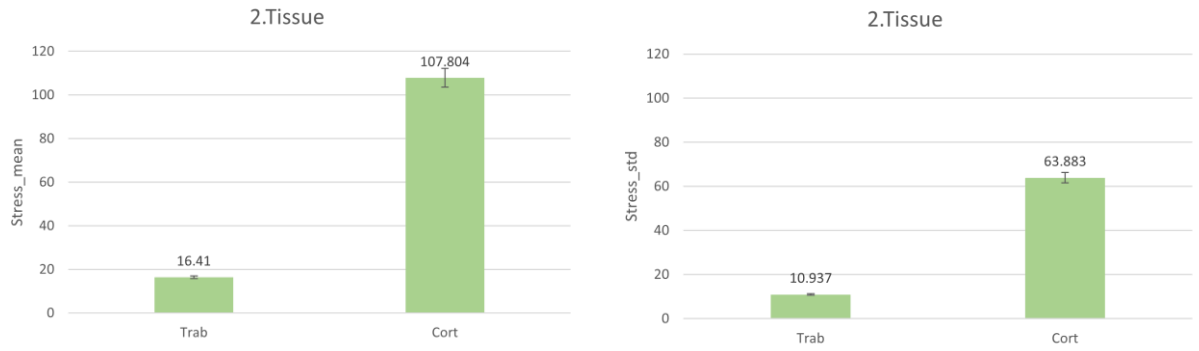

Figure 24:

b)Trochanter analysis on mean value and std of MPS. Estimated mean and std.Error are graphed in relation to the second factor identified by "Tissue" (Trab-Cort).

c)

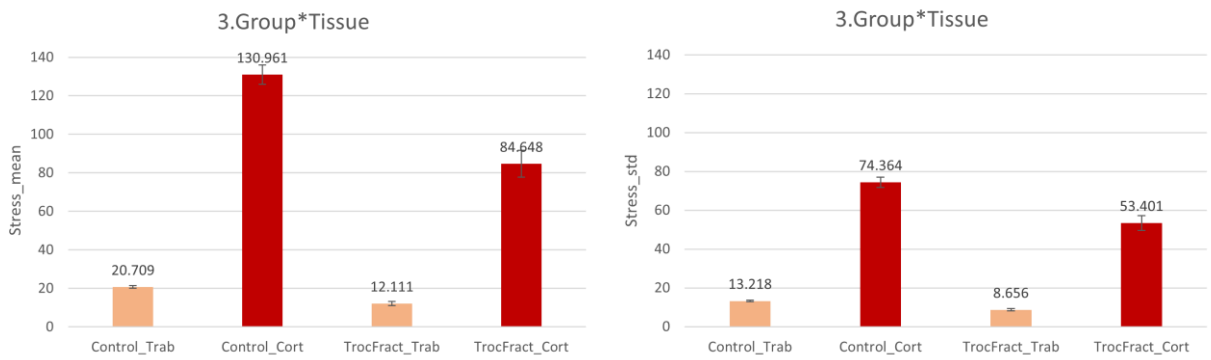

Figure 24:

*c)Trochanter analysis on mean value and std of MPS. Estimated mean and std.Error are graphed in relation to the interaction between factors identified by "Group*Tissue".*

d)

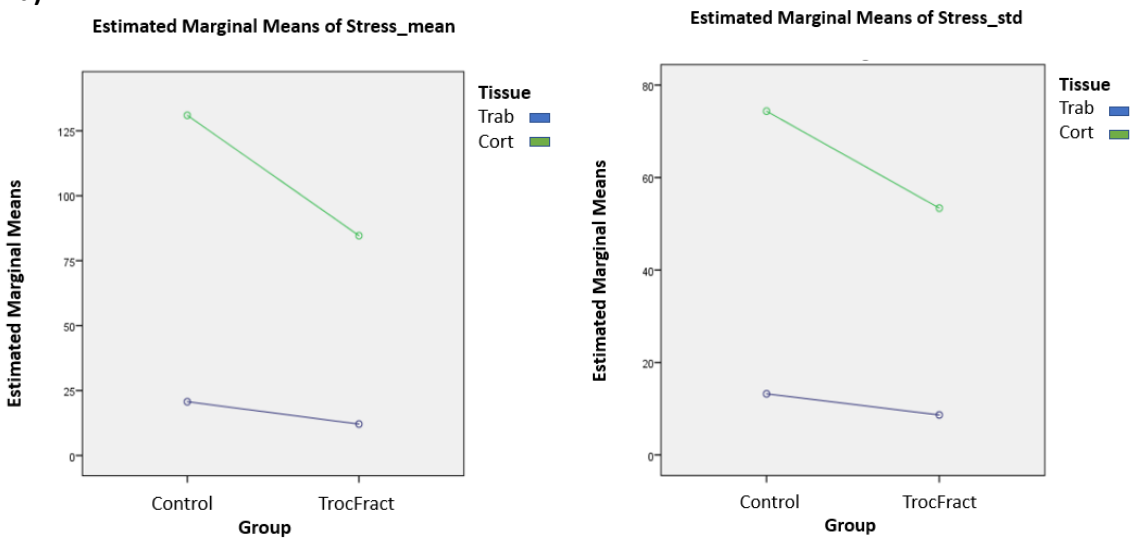

Figure 24:

*d)Trochanter analysis on mean value and std of MPS. Estimated marginal means are graphed in relation to the interaction between factors identified by "Group*Tissue".*

TrocAnalysis				
Stress				
	1. Group	**2. Tissue**	**mean**	**Std.Error**
Stress_mean	Control	Trab	20.709	0.751
		Cort	130.961	4.994
	TrocFract	Trab	12.111	1.048
		Cort	84.648	6.969
Stress_std	Control	Trab	13.218	0.432
		Cort	74.364	2.707
	TrocFract	Trab	8.656	0.603
		Cort	53.401	3.777

Table 11: Trochanter analysis on mean value and std of MPS.

*Estimated marginal means are reported in relation to the interaction between factors identified by "Group*Tissue".*

- **Trochanter Analysis on mean value and std of MPE**

a)

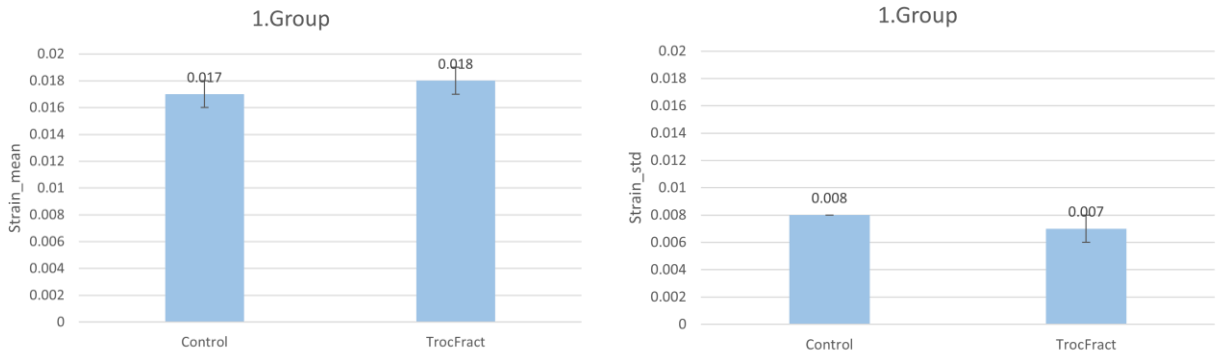

Figure 25:

a)Trochanter analysis on mean value and std of MPE. Estimated mean and std.Error are graphed in relation to the first factor identified by "Group" (Control-TrocFract).

b)

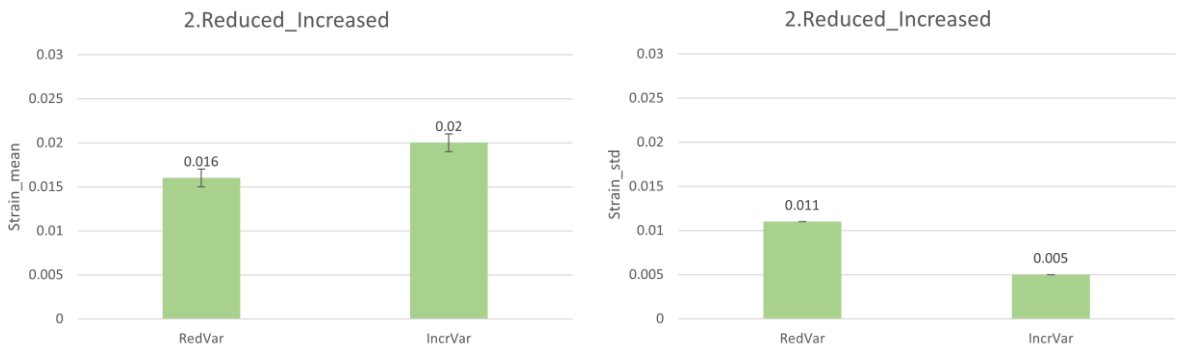

Figure 25:

b)Trochanter analysis on mean value and std of MPE. Estimated mean and std.Error are graphed in relation to the second factor identified by "Reduced_Increased" (RedVar-IncrVar).

c)

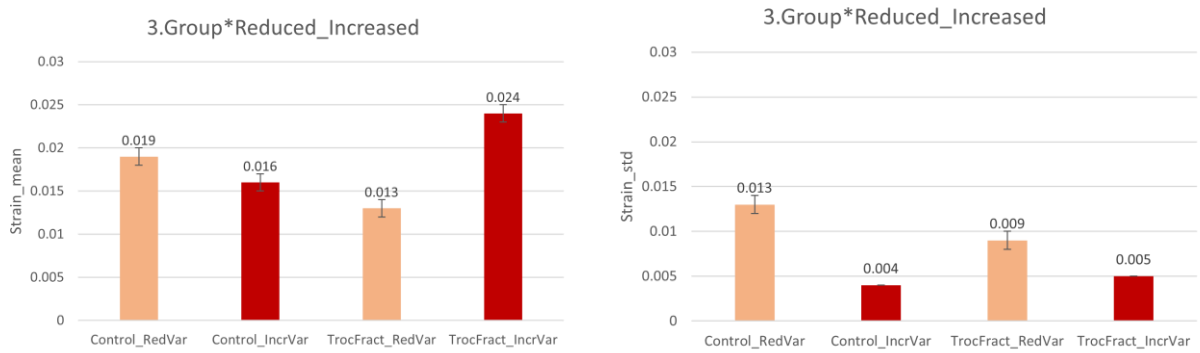

Figure 25:

*c)Trochanter analysis on mean value and std of MPE. Estimated mean and std.Error are graphed in relation to the interaction between factors identified by "Group*Reduced_Increased".*

d)

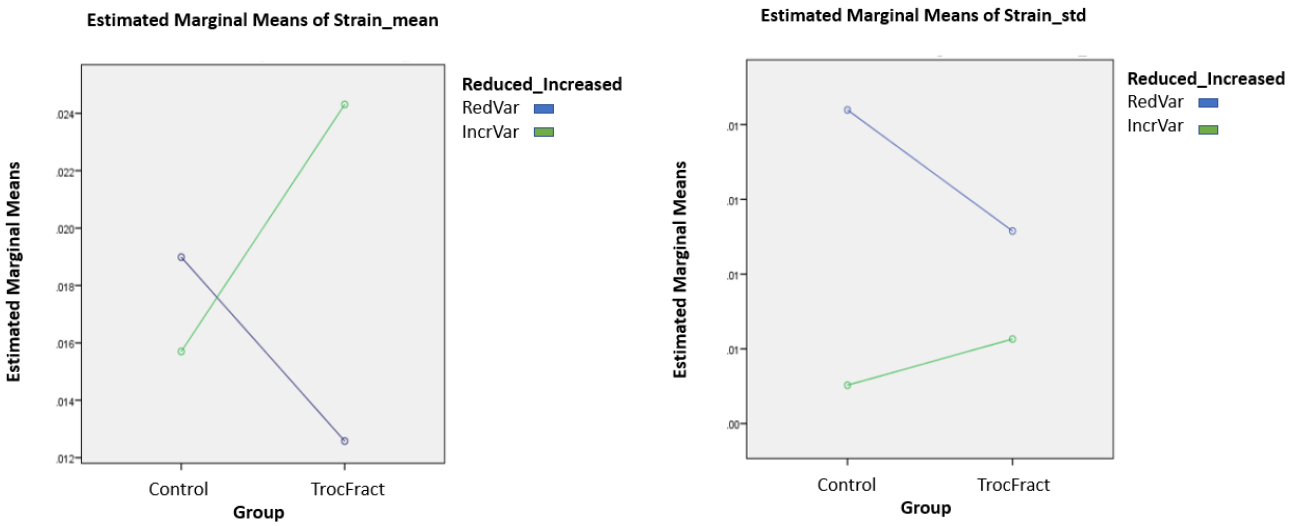

Figure 25:

*d) Trochanter analysis on mean value and std of MPE. Estimated marginal means are graphed in relation to the interaction between factors identified by "Group*Reduced_Increased".*

TrocAnalysis				
Strain				
	1. Group	**2. Reduced_Increased**	**mean**	**Std.Error**
Strain_mean	Control	RedVar	0.019	0.001
		IncrVar	0.016	0.001
	TrocFract	RedVar	0.013	0.001
		IncrVar	0.024	0.001
Strain_std	Control	RedVar	0.013	0.001
		IncrVar	0.004	0.000
	TrocFract	RedVar	0.009	0.001
		IncrVar	0.005	0.000

Table 12: Trochanter analysis on mean value and std of MPE.

*Estimated marginal means are graphed in relation to the interaction between factors identified by "Group*Reduced_Increased".*

3.4 ROC curves

The ROC curves extracted from the two analyses in relation to the whole area of neck and trochanter and belonging to the statistically significant elements respectively, were shown (Fig. 26-27). The area under each curve (AUC) is reported into Tab. 13 and Tab. 14 concerning each independent variable in order to evaluate the discriminant diagnostic power of the two different analyses compared.

- **Neck region**

a)

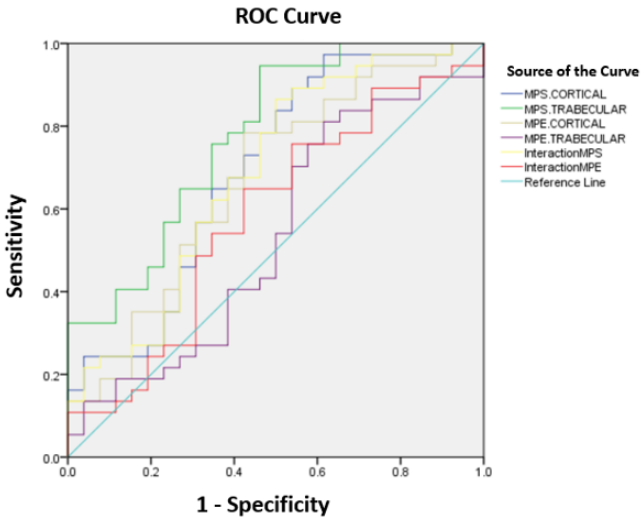

b)

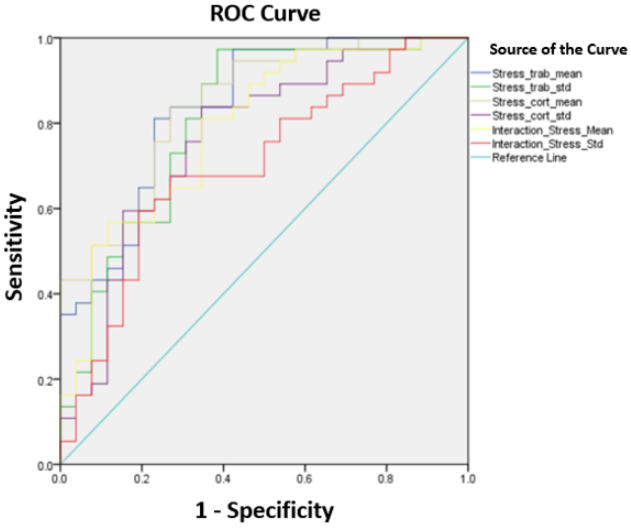

Figure 26:

a)ROC curves concerning neck region in relation to Generation_1.

b)ROC curves concerning neck region in relation to Generation_2.

Area under the Curve	
Test Result Variable(s)	**Area**
MPS.CORTICAL	0.694
MPS.TRABECULAR	0.777
MPE.CORTICAL	0.670
MPE.TRABECULAR	0.534
InteractionMPS	0.686
InteractionMPE	0.583

Area under the Curve	
Test Result Variable(s)	**Area**
Stress_trab_mean	0.838
Stress_trab_std	0.809
Stress_cort_mean	0.844
Stress_cort_std	0.765
Interaction_Stress_Mean	0.790
Interaction_Stress_std	0.702

Table 13:

a)Area under the curve, concerning neck region in relation to Generation_1, obtained for each variable taken into account.

b)Area under the curve, concerning neck region in relation to Generation_2, obtained for each variable taken into account.

- **Trochanter region**

a)

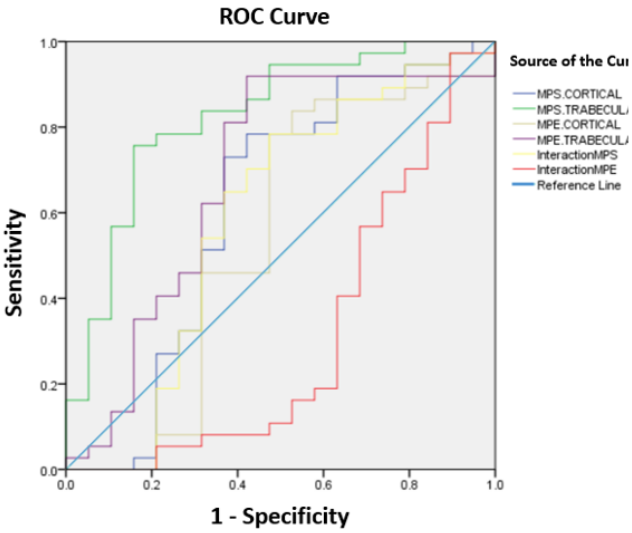

Figure 27:

a)ROC curves concerning trochanter region in relation to Generation_1.

b)

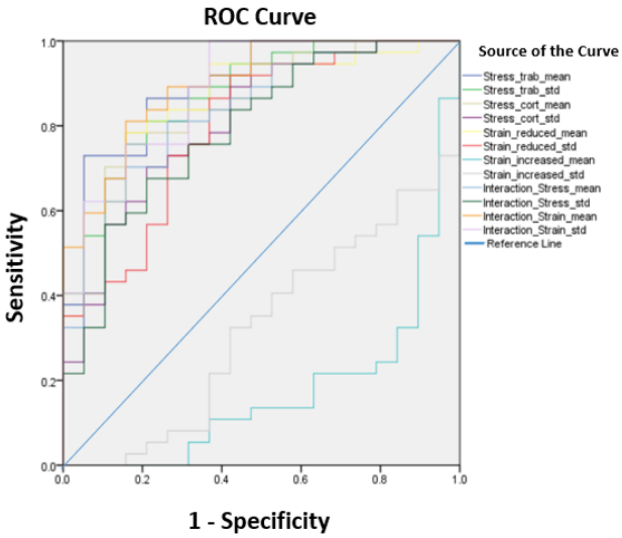

b)ROC curves concerning trochanter region in relation to Generation_2.

Area under the Curve	
Test Result Variable(s)	**Area**
MPS.CORTICAL	0.613
MPS.TRABECULAR	0.825
MPE.CORTICAL	0.541
MPE.TRABECULAR	0.683
InteractionMPS	0.590
InteractionMPE	0.310

Table 14:

a)Area under the curve, concerning trochanter region in relation to Generation_1, obtained for each variable taken into account.

Area under the Curve	
Test Result Variable(s)	**Area**
Stress_trab_mean	0.896
Stress_trab_std	0.871
Stress_cort_mean	0.853
Stress_cort_std	0.812
Strain_reduced_mean	0.855
Strain_reduced_std	0.799
Strain_increased_mean	0.174
Strain_increased_std	0.321
Interaction_Stress_mean	0.834
Interaction_Stress_std	0.791
Interaction_Strain_mean	0.898
Interaction_Strain_std	0.885

b)Area under the curve, concerning trochanter region in relation to Generation_2, obtained for each variable taken into account.

4 Discussion

The research question investigated in this thesis concerns the application of rigorous methodology to identify statistically different areas between controls and fractured patients about hip fracture regions providing a quantitative and qualitative analysis that overcomes the limitation due to the multiple comparison problem in statistics and to the visual identification based on FE model.

4.1 Two-sample t-test: SPMs and test output

The results obtained, graphed in the SPMs (Fig. 20-21) and resumed in the tables of tests outputs (Tab. 6-7), suggests how the dependent variable MPS is dominant compared to the variable MPE. All Two-sample t-tests based on MPS have been produced a rejection of the null hypothesis, it means that there is a difference between the two examined groups, except in the comparison between Fracture_neck_male/Control_male on cortical tissue and between Fracture_trochanter_male/Control_male. However, this result might be related to the small number of male patients and therefore reduced power of the analysis. The tests about the variable MPE have not identified any statistical difference except in the comparison between Fracture_throcanter_female/Control_female belonging to cortical tissue (the same test on the trabecular has not exceeded the threshold).

The results thus demonstrate not only an evident impact of the MPS but provide an additional information about gender: the females represent an important discriminant factor in the comparison between fractures/controls in all tests both on MPS and on MPE. In addition, the SPMs concern the variable MPE on male gender that have not passed the threshold, are much further from the z_star line of SPMs compared with female gender. This is particularly evident in the SPM obtained in the comparison between Fracture_trochanter_male/Control_male. In general, the fact that women, both fractured and controls, are more predisposed to osteoporosis find an agreement with the literature due to a rapid bone loss with aging.

About SPM obtained from Fracture_throchanter_female/Control_female on MPE, it is observed that-test continuum SPM{t} (black line depicted in graph) crosses the

threshold first below and then above. Because the test compares fracture patients with controls, the SPM{t} that exceed the threshold below provides information on the fact that fractured group presents lower values of MPE compared with controls while where the black line overcomes above the threshold it means that fractured group have higher values of MPE respect of controls. In both cases significant clusters are generated. It implies that there are statistically significant regions of cortical tissue in which the MPE decreases and statistically significant regions of cortical tissue in which the MPE increases.

Interesting results about tissue are shown in Tab. 8 and Tab. 9. Based only on the tests belonging to the variable MPS that have produced supra-threshold clusters, the data provide a relatively low percentage of significant elements in relation to the overall elements that constitute the zone of analysis of the FE femur model. It is a confirmation that not the whole area examined can be considered significant as a critical region, although this area includes regions usually subjected to the risk of fractures (neck and intertrochanter). This is less evident in the comparison between Fracture_trochanter_female/Control_female in which the percentage on the total is almost five times bigger than the comparison between Fracture_neck_female/Control_female, although in the comparison concerning Fracture_trochanter_female/Control_female the amount of significant element represents only a 15.96% of the total elements in the zone of analysis. The results therefore demonstrate that it is possible to reduce these regions in a subset of elements that revealed a statistically difference between the investigated groups. In addition, it is observed that the percentage of statistically elements belonging to trabecular tissue is higher than those belonging to cortical tissue.

4.1.1 3D visualization in FE model

Fig. 22 provides a three-dimensional visualization of the critical regions that are the result of the statistical analysis. In this manner is obtained a qualitative and quantitative visualization in terms of significant elements based on a rigorous mathematical approach.

In particular, the image obtained by comparison between Fracture_neck_female/Control_female on MPS shows as critical region not only that represented by elements belonging to the neck with a prevalence at the top, but also elements belonging to the external part of intertrochanter area and just

below to the grand trochanteric area. It means that the test that involves neck fracture patients with control patients does not necessarily imply that the significant elements will have to belong only to the neck region.

In the comparison between Fracture_neck_male/Control male on MPS, indeed, there are also elements in the intertrochanter area although the fractured group is of the neck. An interesting finding is about the significant elements belonging to the Fracture_neck_male group for which it has been found that the elements represent a subset of the significant elements detected in the Fracture_neck_female_group.

Observing the significant elements obtained by Fracture_trochanter_female/Control_female test, on MPS variable, is noted that a larger number of significant elements is located in the trabecular tissue in the upper part of the neck and above all in greater trochanter area; also, the lower part of proximal femur is involved. About the cortical tissue, the significant elements cover the bottom of the neck and a large area of the intertrochanter down to the base of the proximal femur.

Very similar is the situation obtained on MPE variable, concerning the cortical tissue. In the trabecular tissue no significant elements are detected.

4.2 Second level analysis: Two-way ANOVA with repeated measures

To investigate deeper the dependent variable (MPS/MPE) in relation to significant elements obtained, the mean value and std for each type of tissue have been considered for each patient belonging to each group (Appendix I) and used for Two-way ANOVA with repeated measures analyses. Only female gender has been considered.

This type of analysis is to be considered complementary to the Two-sample t-test because, although is less refine than the previous analysis based on the dependent variable associated element by element, provides us a global statistic

vision using estimated marginal means. Therefore, the multifactorial analysis makes it possible to resume in appropriate graphs and tables, immediately understandable, if compared with the graphical visualization of statistical elements in the FE model.
Moreover, it allows us to compare the analysis performed during this work with more traditional analysis performed over the global zones presented previously and shown to the side (Fig. 28).

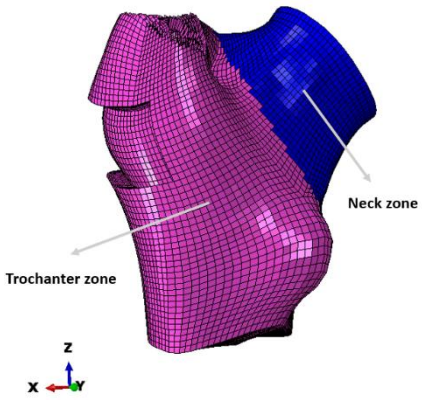

Figure 28: Zone of analysis

The results, depicted in the bar charts (Fig. 23-24-25) and reported in the tables of Appendix II section, shown a different scenario for each of three multifactorial analyses computed:

1. *Neck Analysis on mean value and std of MPS:*

   About the first factor, represented by “Group” (Control-NeckFract), the estimated mean in relation both Stress_mean and Stress_std is noted greater in controls than fractured. The higher values of standard deviation indicate that the fractured group have a lower variability (Fig. 23 (a).

   The second factor, the “Tissue” (Trab-Cort), shows an estimated mean of the stress bigger for both mean and standard deviation in relation to cortical tissue. This is not surprising and can be related to the different composition and mechanical behaviour of trabecular and cortical bone, in accord with literature (Fig. 23 (b).

   The interaction between factors “Group*Tissue” (Control-NeckFract; Trab-Cort) reported in Tab. 10, is better identified by observing the bar chart in Fig. 23 (c simultaneously with Fig. 23 (d.
   The image about Stress_mean shows a decreased in both tissue passing from control group to neck fracture group with value of estimated marginal means bigger for cortical tissue, as we expected. However, values of estimated marginal means decrease more in cortical tissue than trabecular tissue.

The situation is similar in the image in which the Stress_std is shown. Although the Stress_std for both tissues decrease passing from control group to neck fracture group, the decrement is comparable but still statistically significant since the interaction is significant in both tissues, with a slight greater slope in cortical tissue.

To better discriminate between fracture and control subjects it has been created a new variable of the difference based on estimated marginal means belonging to different tissues. Where the difference is high the patient can be defined as neck fractured, otherwise control.

2. *Trochanter Analysis on mean value and std of MPS:*

In this case, the first factor, the “Group” (Control-TrocFract), shows the estimated mean about Stress_mean and Stress_std bigger in the control group than fractured group. The standard deviation is once again greater in control patients, which have a greater variability (Fig. 24 (a).

Similar to the neck analysis about the second factor, the “Tissue” (Trab-Cort), the estimated mean in relation to cortical tissue is bigger in cortical tissue for both Stress_mean and Stress_std, as was to be expected. While the std.Error is higher in cortical tissue, but in this case is more evident than neck analysis (Fig. 24 (b).

The interaction between factors “Group*Tissue” (Control-TrocFract; Trab-Cort) is reported in Tab. 11 and graphed in Fig. 24 (c (d.
In the image about Stress_mean, the estimated marginal means varies in similar way of neck analysis but with a more pronounced decrease in cortical tissue.
Also, the image concerning the Stress_std shows a decrease for both tissues passing from control group to trochanter fracture group with a high slope in cortical tissue.

Also in this case a new variable of the distance between the estimated marginal means has been created, to better discriminate trochanter fracture patients and controls both for Stress_mean and for Stress_std.

3. *Trochanter Analysis on mean value and std of MPE:*

Observing the first factor “Group” (Control-TrocFract) the estimated mean of Strain_mean and Strain_std is very similar, slightly greater in fractured group, although in both cases significant. The std.Error is the same for both groups about the Strain_mean while the std.Error about Strain_std in relation to the fractured is bigger than control patients, where it is zero (Fig. 25 (a).

About the second factor, “Reduced_Incresed” (RedVar-IncrVar), the estimated mean on the variable Strain_mean is greater for the cortical regions in which the strain increase (IncrVar) compared with the cortical regions in which the strain decrease (RedVar). While is the opposite on the variable Strain_std. About the std.Error it is noted that the Strain_mean is equal for both regions in which the dependent variable decreases and increases, while about the Strain_std is zero for both (Fig. 25 (b).

In the end, the interaction between factors, “Group*Reduced_Increased”, is better explained by observing Fig. 25 (c (d and Tab. 12.
The image concerning the Strain_mean shows an increase of the estimated marginal means passing from control group to trochanter fracture group in the cortical regions characterized by a decrease of strain while shows a decrease of the estimated marginal means in the cortical regions in which the variable strain increases. The interesting thing is that the estimated marginal means is very similar in controls for both cortical regions, greater for regions with high value of strain, while in the trochanter fracture group is the opposite and with much more detached than controls.
The image about the Strain_std depicts a decrease of estimated marginal means passing from control group to trochanter fracture group in relation to the regions in which the strain increases. On the other side, the estimated marginal means, in the regions characterized by a decrease of strain, increase passing from controls to fracture patients.

In general, standard deviation within the selected area is smaller in the fracture population. This result sounds against common beliefs that suggest a healthy tissue to behave uniformly. However, several dynamic approach analyses have suggested how a good degree of variability might be healthy for the tissue and a reduction of this variability might lead to injuries or pathological situations.

4.3 Comparison and ROC curves

To evaluate the accuracy of the tests performed in the present thesis the ROC curves were plotted in comparison with those derived from tests conducted in a previous study in which all elements belonging to the neck and trochanter were considered. So, by comparing the two analyses to establish the measure of how well a parameter can distinguish between two diagnostic groups (fractured/control) the Area Under the ROC curve (AUC) was considered.

- *Neck region*

Observing the ROC curves belonging to Generatin_1 and Generation_2 (Fig. 26 (a (b) with Tab. 13 (a (b, it is evident that the AUC values associated to each parameter of interest are closer to 1 in Generation_2 than Generation_1. It means the model discussed in this thesis has a good measure of separability between fracture and control group in relation to the neck region than the previous study. In particular, the Generation_2 has a minimum and maximum value of AUC equal to 0.7655 and 0.844 respectively against the 0.534 and 0.777 belonging to Generation_1. In addition, the Generation_1 presents two different variables (MPE.TRABECULAR and InteractionMPE) for which the AUC is roughly equal to 0.5. It means that the model has no class separation capacity.

- *Trochanter region*

Also in this case, how it is shown in Fig. 27 (a (b in relation to Tab. 14 (a (b, the AUC values are greater in Generation_2, of which only a variable presents an AUC under 0.6 (Strain_increased_std). By contrast, Generation_1 features AUC not higher than 0.69 with the only exception of MPS.TRABECULAR variable (0.825). In general, it means that the model of the present thesis has a greater discriminating power between the investigated group.

4.4 Limitations

The reliability of results is impacted by how the 1D trajectory has been built. Although the algorithm implemented proceeds properly in the junction of reference nodes based on minimum distance, it has been detected a first limitation when a specific condition is met.

In detail (Fig. 29), when the algorithm reveals only one minimum distance between last reference node belonging to the path and one of the remaining nodes not yet selected, the junction procedure is correctly verified (1→2→3→4→5). By contrast, in the case even that one or more minimum distances are detected, it means that different reference remaining nodes have the same distance from the last node in the trajectory (although their spatial location is clearly different) (5→6; 5→11), the algorithm will choose to join arbitrarily only one of them (5→6) and then continue with the calculation of the new minimum distance starting from the last, just joined, node in the trajectory (6). This doesn't imply that the reference nodes with the same distance, which have not been chosen (11), will be the next to join (6→7) because of the minimum distance. In that case, the algorithm regularly proceeds (7→8→10) but at one point it will have to join these remaining nodes, although they seem so far away, therefore producing undesirable but inevitable spatial jumps in the 1D trajectory.

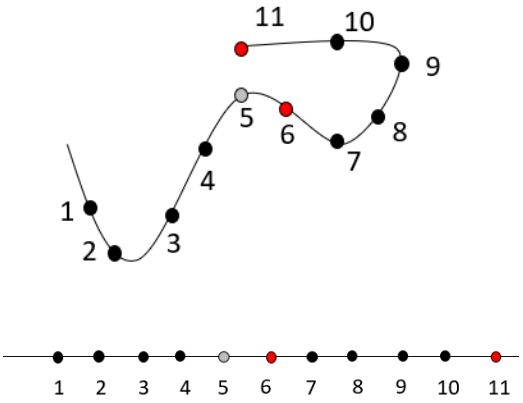

Figure 29: Relation between spatial location of nodes and order sequence of nodes in the 1D trajectory.

It is impossible to avoid this situation because at the end of this procedure all nodes will have to be connected in a unique trajectory. Fig. 29 shows the final trajectory obtained and, as we expected, there are nodes along the path located in distant positions (points 6 and 11), despite they are spatially very close.

In this regard, future researchers could take into account this phenomenon evaluating the possibility to implement optimization procedures of the algorithm

presented in this thesis. However, these events are limited and in general the identified regions are coherent, showing that, as a general rule, points that might be far away in the 1D trajectory, but close in the 3D space, are actually identified together.

A second limitation is due to the impossibility to conduct a Two-way ANOVA with repeated measures using the software “spm1d” and therefore the application of RFT. This type of statistical test is included in the package but unfortunately it does not allow to process unbalanced data. In our specific case the number of elements of the femur model belonging to each patient is always the same for FE construction, the same goes for the type of tissue, which is trabecular or cortical. What makes unbalanced data is the different number of patients for each investigated group (26 Fracture_neck_female, 19 Fracture_trochanter_female, 37 Control_female, 10 Fracture_neck_male, 7 Fracture_trochanter_male, 12 Control_male). For this reason, future studies should increase the number of patients making the number of subjects for each category balanced.

Last limitation is the lack of male patients in the dataset used in this study (10 neck fracture subjects, 7 trochanter fracture subjects and 12 controls). This deficiency led to exclude male gender in the second level analysis, although the Two-sample t-test had produced statistically significant elements in the comparison between Fracture_neck_male/Control_male in relation to trabecular tissue. In general, it is advised to include a larger number of male patients to have more reliable results.

5 Conclusion

The research aimed to identify statistically significant differences between fractured and control groups, with the purpose of determining potential critical regions where proximal femur fracture may occur due to later falls.

The rigorous methodology implemented has revealed interesting findings leading us to conclude that the region in which fracture happens doesn't necessarily represent the zone detected as statistically significant. Have in fact been identified significant elements in the neck region, although the investigated group was fractured in the trochanter, and vice versa. In addition, the local nature of the critical region was confirmed, being involved only a small percentage of significant elements in the FE model (less than 10%). This phenomenon is evident on the improvement of classification results, which demonstrates positive effects as a consequence of the reduction of the zone of analysis compared with the whole proximal femur.

Another important discovery reveals the variable MPS as most meaningful, with higher values of mean_Stress in the controls than fractured. An interesting finding is the variability, lower in fractured patients, which suggests new cues of reflection contrary to common conception concerning the homogeneous mechanical behaviour of healthy bone. In fact, reduced variability for the fractured subjects suggests a more homogeneous behaviour for fractured subjects, while higher variability of the control subjects might be in accordance with the fact that distributed stimuli induce bone remodelling and consequently a decrease of osteoporotic fracture risk.

In the end, the ROC curves in relation to the Generation_2 (only statistically significant element belonging to neck and trochanter were considered) presented in this thesis have been showed higher AUC values meaning that the discriminant power of tests, in term of accuracy, is better than the previous study concerning the Generation_1 (all elements belonging to neck and trochanter were considered).

In the light of scientific findings just outlined, the present thesis provides a relevant contribution towards the development of biomechanical and clinical research, that may be further explored and investigated.

6 Bibliography

[1] Sànchez-Riera L., & Wilson N., *Fragility Fractures & Their Impact on Older People*. Best Practice and Research: Clinical Rheumatology (2017); 31(2), 169-191. https://doi.org/10.1016/j.berh.2017.10.001

[2] Eyüboğlu F., Sayaca Ç., et al., *Kinesiology of the hip*. Comparative Kinesiology of the Human Body (2020); 375-392.

[3] NIH Consensus Development Panel on Osteoporosis Prevention, Diagnosis, and Therapy. *Osteoporosis prevention, diagnosis, and therapy*. JAMA (2001); 285(6):785-795.

[4] Dobbs M.B., Buckwalter J., et al., *Osteoporosis: the increasing role of the orthopaedist*. The Iowa orthopaedic journal (1999); 19:43-52. PMID: 10847516; PMCID: PMC1888612.

[5] Thomas T.N*., Lifestyle risk factors for osteoporosis*. Medical-surgical Nursing Journal (1997); 6(5):275-7, 287. PMID: 9384153.

[6] Crabtree N., Loveridge N., et al., *Intracapsular hip fracture and the region-specific loss of cortical bone: Analysis by peripheral quantitative computed tomography*. Journal of Bone and Mineral Research (2001); 16(7), 1318-1328. https://doi.org/10.1359/jbmr.2001.16.7.1318

[7] Campbell W.C., Canale S.T., et al., *Fractures and dislocations of the hip*. Campbell's Operative Orthopaedics. 11th ed. Phildelphia, PA: Mosby/Elsevier (2008); 3237-3283.

[8] Hernlund E., Svedbom A., et al., *Osteoporosis in the European Union: medical management, epidemiology, and economic burden. A report prepared in collaboration with the International Osteoporosis Foundation (IOF) and the European Federation of Pharmaceutical Industry Associations (EFPIA).* Archives of Osteoporosis (2013); 8:136.

[9] Rizzoli R., *Postmenopausal osteoporosis: Assessment and management*. Best Practice & Research Clinical Endocrinology & Metabolism (2018); *32*(5), 739-757. https://doi.org/10.1016/J.BEEM.2018.09.005

[10] LeBlanc E.S., Hillier T.A., et al*., Hip fracture and increased short-term but not long-term mortality in healthy older women*. Archives of Internal Medicine (2011); 171(20):1831-1837.

[11] Haentjens P., Magaziner J., et al., *Meta-analysis: excess mortality after hip fracture among older women and men.* Annals of Internal Medicine. (2010); 152(6): 380-390.

[12] Landefeld C.S., *Goals of care for hip fracture: promoting independence and reducing mortality*. Archives of Internal Medicine (2011); 171(20):1837-1838.

[13] Kanis J.A., Odén A., et al., IOF Working Group on Epidemiology and Quality of Life. *A systematic review of hip fracture incidence and probability of fracture worldwide*. Osteoporosis International (2012); 23(9):2239-56. doi: 10.1007/s00198-012-1964-3

[14] Brett M., Penny W., et al., *Introduction to Random Field Theory*. Human Brain Function, 2th ed. (2003); 867-879.

[15] Kiebel S.J., Poline J.B., et al., *Robust smoothness estimation in statistical parametric maps using standardized residuals from the general linear model*. NeuroImage (1999); 10:756-766.

[16] Worsley K.J., Andermann M., et al., *Detecting changes in nonisotropic images*. Human Brain Mapping (1999); 8:98-101.

[17] Worsley K.J., Evans A.C., et al., *A three-dimensional statistical analysis for CBF activation studies in the human brain*. Journal of Cerebral Blood Flow and Metabolism (1992); 12:900-918.

[18] Brett M., Penny W., et al., *Parametric procedures*. Statistical Parametric Mapping: The Analysis of Functional Brain Images (2007); 223-231.

[19] Sievanen H., Oja P., et al., *Precision of dual-energy x-ray absorptiometry in determining bone mineral density and content of various skeletal sites*. Journal of Nuclear Medicine (1992); 33(6), 1137-1142.

[20] Ott S.M., O'Hanlan M., et al., *Evaluation of vertebral volumetric vs. areal bone mineral density during growth*. Bone (1997); 20(6), 553-556.

[21] Genant H.K., Block J.E., et al., *Quantitative computed tomography in assessment of osteoporosis*. Seminars in Nuclear Medicine (1987); 17(4):316-33.

[22] Unnanuntana A., Gladnick B.P., et al., *The assessment of fracture risk*. The Journal of bone and joint surgery (2010); *92*(3), 743-753.

[23] Abrahamsen B*., FRAX® in clinical practice*. Nature Reviews Rheumatology (2011); 686-688.

[24] Wainwright S.A., Marshall L.M., et al., *Hip fracture in women without osteoporosis*. Journal of Clinical Endocrinology & Metabolism (2005); 90:2787-93.

[25] Grassi L., Väänänen S.P., et al., *Prediction of femoral strength using 3D finite element models reconstructed from DXA images: validation against experiments.* Biomechanics and Modelling in Mechanobiology *(2017)*; *16*(3), 989-1000.

[26] Keaveny T.M., Kopperdahl D.L., et al., *Age-dependence of femoral strength in white women and men*. Journal of Bone and Mineral Research (2010); 25:994-1001.

[27] Keyak J.H., Sigurdsson S., et al., *Male-female differences in the association between incident hip fracture and proximal femoral strength: A finite element analysis study*. Bone (2011); 48:1239-45.11.

[28] Keaveny T.M., Hoffmann P.F., et al., *Femoral bone strength and its relation to cortical and trabecular changes after treatment with PTH, alendronate, and their combination as assessed by finite element analysis of quantitative CT scans*. Journal of Bone and Mineral Research (2008); 23:1974–82.12.

[29] Naylor K.E., McCloskey E.V., et al., *Use of DXA-based finite element analysis of the proximal femur in a longitudinal study of hip fracture*. Journal of Bone and Mineral Research (2013); 28(5):1014-21. doi: 10.1002/jbmr.1856. PMID: 23281096

[30] Tassani S., Pani M., Noailly J., et al., *Trabecular fracture zone might not be the higher strain region of the trabecular framework.* Frontiers in Materials (2018); 1-9.

[31] Tassani S., Matsopoulos G.K., et al., *3D identification of trabecular bone fracture zone using an automatic image registration scheme: A validation study*. Journal of Biomechanics (2012); 45(11):2035-40. doi: 10.1016/j.jbiomech.2012.05.019

[32] Ruiz Wills C., Tassani S., et al., *Relative fragility of osteoporotic femurs assessed with DXA and simulation of finite element falls guided by emergency X-rays.* Revista de Osteoporosis y Metabolismo Mineral (2020); 12(2), 62-70. https://doi.org/10.4321/S1889-836X2020000200005

[33] Ruiz Wills C., Olivares A.L., Tassani S., et al., *3D patient-specific finite element models of the proximal femur based on DXA towards the classification of fracture and non-fracture cases.* Bone (2019); 89-99. https://doi.org/10.1016/j.bone.2019.01.001

[34] Pataky T.C., *One-dimensional statistical parametric mapping in Python.* Computer Methods in Biomechanics and Biomedical Engineering (2012); *15*(3), 295-301. https://doi.org/10.1080/10255842.2010.527837

[35] Adler R.J., *The geometry of random fields*. New York: Wiley (1981).

[36] Friston K.J., Frith C.D., et al., *Comparing functional (PET) images: the assessment of significant change*. Journal of cerebral blood flow and metabolism: official journal of the International Society of Cerebral Blood Flow and Metabolism (1991); 11:690-699.

[37] Friston K.J., Worsley K.J., et al., *Assessing the significance of focal activations using their spatial extent.* Human Brain Mapping, (1994); 1:214-220.

[38] Worsley K.J., Marrett S., et al., *A unified statistical approach or determining significant signals in images of cerebral activation*. Human Brain Mapping *(1996)*; 4:58-73.

[39] Pataky T.C., *rft1d: Smooth one-dimensional random field upcrossing probabilities in Python*. Journal of Statistical Software (2016); 71(7). https://doi.org/10.18637/jss.v071.i07

7 Acknowledgements

I would like to offer my sincere thanks to my internal supervisor Lorenzo Peroni for having accepted the proposed thesis request, for the support and for trusting me during the six months abroad.

I would like to express my gratitude to my tutors Simone Tassani and Carlos Ruiz Wills, who guided and supported me throughout the entire project providing me precious suggestions and encouragement at every stage of the thesis.

I wish to acknowledge the help provided by Politecnico di Torino, for having made possible this formative experience of exchange abroad, and also the host university UPF of Barcelona with a special thanks to Jérôme Noailly and the entire Computational Biomechanics and Mechanobiology group that supported me weekly during the project.

A sincere thank goes to Laura, colleague and friend, for her deep insight with whom I shared difficult and beautiful moments, and long good chats during daily coffee breaks and meals.

My heartfelt thanks to my parents, Daniela and Giuseppe, for their unwavering support and belief in me. I would also like to thank my siblings Federica and Luca, my grandparents and all my family for always having been, even at a distance.

I would like to thank my special friend Valeria, with whom I have spent last years of my university studies. She always there for me and I never forget all the moments lived together through joys and sorrows.

A huge thanks to all my friends of Torino and in special way to Margherita, Mirella, Francesca, Roberta, Giulia, Massa, Christian, Mattia, Matteo and Alberto. They are my second family, lovely people and real friends.

I cannot fail to thank my historical friends Marzia, Irene and Carla, ever present in each moment of my life, always by my side and there to pick me up.

A special thank goes to Chiara, Elisabetta and Benedetta on which I can always count on, although often there has been great distance from each other in recent years but never enough!

Thanks to Marcello, with whom I shared both moments of stress and light-heartedness, having in common a great desire to do a good work.

I would like to thank Louis for being so patient especially during the months in Barcelona and for having always believed in me.

A special word of thanks to all my roomies and in particular to Marica, Anna, Maria, Manuela, Valeria, Gianna, Gabri and “Les serfeur de la night”, who I love very much and for which I could not have wished for a better togetherness.

Appendix I

- Major Principal Stress (MPS)

CONTROL_FEMALE					
	ID PATIENT	TRABECULAR		CORTICAL	
		mean	std	mean	std
MPS	361418	23.603	15.858	79.535	48.375
	1547561	18.168	15.688	79.335	37.379
	1861487	22.265	15.263	95.130	37.080
	2213332	16.406	12.349	73.272	30.721
	2797349	18.595	14.588	76.215	39.602
	3144605	16.420	11.216	58.921	31.160
	3159064	26.518	16.406	84.344	44.236
	4106200	17.856	11.901	71.073	28.222
	15388207	20.809	18.647	77.891	45.456
	25088216	21.038	15.351	70.091	45.048
	29754300	19.212	13.176	77.645	31.405
	39923300	12.601	11.139	65.671	25.317
	43850215	16.555	11.857	68.846	32.997
	49599206	24.403	15.920	73.516	39.737
	64965310	24.241	18.257	73.152	35.947
	68849206	20.645	19.254	97.446	44.168
	73019200	22.942	14.500	63.805	36.146
	77750514	16.103	12.850	78.680	33.642
	79701814	20.996	13.950	69.124	34.951
	89122200	19.927	15.506	80.818	36.786
	97481706	19.176	14.686	80.764	37.239
	98956212	17.878	15.189	61.522	37.231
	152587905	12.070	10.746	80.241	25.215
	171209714	19.449	15.140	101.495	42.162
	203439500	17.507	13.989	83.075	32.641
	217553200	9.882	10.427	51.491	30.228
	242713704	17.470	12.942	76.703	39.411
	291747904	11.654	7.634	46.860	21.918
	304408700	17.167	14.280	76.315	37.716
	312500202	23.137	15.307	72.713	36.230
	314821503	12.159	11.093	72.977	24.040
	315298200	20.051	16.710	62.171	36.256
	315504300	20.551	13.488	63.166	29.142
	320462200	12.867	10.562	59.657	27.282
	321882600	22.715	15.413	86.854	35.520
	321950400	18.664	13.605	82.426	31.494
	327485900	21.118	13.506	89.330	40.702

FRACTURE_NECK_FEMALE					
	ID PATIENT	TRABECULAR		CORTICAL	
		mean	std	mean	std
MPS	13619803	9.362	9.224	48.287	23.958
	23245811	5.296	7.267	42.371	26.569
	67023402	13.036	12.731	46.514	30.916
	70241012	11.210	9.923	47.222	31.541
	99215805	8.552	9.263	38.700	23.195
	160982300	17.570	16.111	73.136	44.229
	165056200	20.160	13.895	77.096	36.272
	165148802	20.589	15.626	73.157	40.463
	189418300	11.023	10.337	53.017	19.012
	191921515	4.052	5.950	39.624	17.671
	207413604	19.137	9.761	73.646	24.059
	254489000	6.219	8.384	45.471	23.505
	280142403	11.434	8.575	52.337	27.703
	285965700	7.613	8.147	44.306	27.120
	286805800	10.840	10.301	76.086	29.134
	320934500	6.068	6.757	50.647	17.618
	321312300	13.539	11.514	54.328	28.111
	321346601	8.803	7.889	51.089	23.786
	322650000	11.431	9.364	66.571	28.281
	323223100	14.023	10.884	40.056	28.387
	323369700	16.216	14.490	62.267	34.481
	323524400	10.101	8.959	61.225	20.822
	323706901	19.665	15.001	58.131	41.613
	325162501	19.319	13.826	62.648	33.648
	327585100	14.587	13.779	76.816	33.036
	327738000	9.643	8.097	61.289	25.644

CONTROL_MALE					
	ID PATIENT	TRABECULAR		CORTICAL	
		mean	std	mean	std
MPS	35828027	12.871	5.635		
	45311500	10.089	4.466		
	98044100	13.666	6.376		
	204727302	11.306	6.355		
	224355512	13.896	7.682		
	301035802	7.953	3.683		
	319961000	14.416	7.327		
	324719500	9.223	4.296		
	325619100	14.519	9.029		
	326817500	12.144	7.025		
	327013200	13.923	7.344		
	327412001	14.807	7.778		

FRACTURE_NECK_MALE					
	ID PATIENT	TRABECULAR		CORTICAL	
		mean	std	mean	std
MPS	38397800	4.454	2.900		
	49466603	11.274	5.761		
	74065000	5.300	3.070		
	150972201	8.220	4.517		
	249733100	5.070	2.525		
	266077700	3.555	2.222		
	279074500	5.325	3.186		
	289977301	5.389	3.015		
	328365600	3.587	1.843		
	329192100	3.433	1.648		

CONTROL_FEMALE					
	ID PATIENTS	TRABECULAR		CORTICAL	
		mean	std	mean	std
MPS	361418	27.890	16.883	169.641	97.778
	1547561	20.372	13.401	142.908	73.566
	1861487	20.040	12.450	116.806	67.390
	2213332	18.977	12.791	136.341	75.999
	2797349	16.944	11.422	111.006	71.113
	3144605	12.044	7.847	58.812	45.162
	3159064	26.565	16.130	159.097	86.485
	4106200	13.975	9.623	86.894	53.614
	15388207	24.871	16.403	161.840	108.971
	25088216	25.185	15.132	155.848	96.750
	29754300	24.030	15.974	160.059	94.129
	39923300	17.688	11.177	101.248	58.226
	43850215	17.916	10.123	92.539	63.116
	49599206	24.683	14.253	136.143	79.494
	64965310	24.679	16.610	172.323	91.263
	68849206	20.326	15.418	167.206	84.748
	73019200	22.244	13.625	136.007	78.509
	77750514	19.416	13.916	153.023	76.810
	79701814	20.458	12.840	109.892	72.541
	89122200	23.799	14.300	140.849	78.649
	97481706	25.545	16.406	172.060	92.386
	98956212	20.125	13.783	142.174	83.111
	152587905	19.633	12.800	118.957	55.254
	171209714	24.072	14.902	171.908	90.151
	203439500	19.749	12.387	124.253	64.719
	217553200	12.142	9.377	102.022	56.624
	242713704	23.396	14.963	159.108	89.904
	291747904	11.915	6.996	70.059	39.277
	304408700	20.425	14.587	140.942	80.863
	312500202	27.690	15.545	144.614	78.797
	314821503	17.068	12.757	120.399	53.808
	315298200	25.987	15.900	139.884	82.757
	315504300	17.470	10.173	88.586	53.311
	320462200	15.915	9.676	94.546	54.230
	321882600	20.712	12.145	112.927	72.141
	321950400	18.732	12.564	120.722	65.300
	327485900	23.535	13.789	153.919	84.531

FRACTURE_TROCHANTER_FEMALE					
	ID PATIENT	TRABECULAR		CORTICAL	
		mean	std	mean	std
MPS	8799900	12.213	9.648	108.722	57.672
	23505027	12.415	9.158	96.945	53.618
	75004102	6.403	5.148	46.794	26.797
	79030800	23.375	13.961	142.084	85.365
	99151806	18.135	12.934	115.116	72.944
	99458007	14.197	10.421	109.597	65.080
	153229400	8.708	7.439	59.020	48.310
	176038902	6.531	5.583	56.666	41.112
	183772502	8.074	6.805	75.317	49.923
	183843600	18.045	10.095	98.995	64.600
	184256103	7.332	5.030	45.065	30.925
	268606704	9.886	7.949	84.352	51.416
	321555600	9.389	6.811	67.615	43.691
	322029601	8.307	6.284	52.068	37.064
	322806601	18.616	11.454	93.687	71.167
	322939900	16.848	10.248	104.087	61.131
	326296201	16.060	12.764	141.742	80.644
	326855900	7.244	5.409	50.412	32.660
	327569400	8.323	7.332	60.027	40.509

- Major Principal Strain (MPE)

CONTROL_FEMALE →exceeding threshold below					
	ID PATIENT	TRABECULAR		CORTICAL	
		mean	std	mean	std
MPE	361418			0.022	0.016
	1547561			0.025	0.017
	1861487			0.019	0.011
	2213332			0.020	0.014
	2797349			0.018	0.015
	3144605			0.008	0.006
	3159064			0.026	0.018
	4106200			0.015	0.008
	15388207			0.023	0.017
	25088216			0.022	0.017
	29754300			0.023	0.013
	39923300			0.013	0.009
	43850215			0.013	0.011
	49599206			0.021	0.016
	64965310			0.024	0.018
	68849206			0.025	0.016
	73019200			0.016	0.013
	77750514			0.022	0.012
	79701814			0.018	0.013
	89122200			0.022	0.015
	97481706			0.025	0.018
	98956212			0.020	0.016
	152587905			0.015	0.008
	171209714			0.026	0.014
	203439500			0.018	0.012
	217553200			0.017	0.012
	242713704			0.023	0.017
	291747904			0.009	0.007
	304408700			0.021	0.015
	312500202			0.018	0.013
	314821503			0.018	0.010
	315298200			0.017	0.013
	315504300			0.013	0.009
	320462200			0.013	0.010
	321882600			0.018	0.012
	321950400			0.017	0.009
	327485900			0.018	0.012

FRACTURE_TROCHANTER_FEMALE →exceeding threshold below					
	ID PATIENT	TRABECULAR		CORTICAL	
		mean	std	mean	std
MPE	8799900			0.013	0.008
	23505027			0.012	0.007
	75004102			0.008	0.005
	79030800			0.017	0.014
	99151806			0.020	0.013
	99458007			0.016	0.014
	153229400			0.012	0.009
	176038902			0.009	0.008
	183772502			0.011	0.007
	183843600			0.013	0.010
	184256103			0.008	0.005
	268606704			0.011	0.008
	321555600			0.010	0.006
	322029601			0.007	0.006
	322806601			0.014	0.012
	322939900			0.015	0.011
	326296201			0.021	0.015
	326855900			0.009	0.005
	327569400			0.010	0.006

CONTROL_FEMALE →exceeding threshold above					
	ID PATIENT	TRABECULAR		CORTICAL	
		mean	std	mean	std
MPE	361418			0.014	0.004
	1547561			0.009	0.001
	1861487			0.021	0.005
	2213332			0.016	0.005
	2797349			0.030	0.007
	3144605			0.018	0.002
	3159064			0.013	0.003
	4106200			0.024	0.004
	15388207			0.016	0.005
	25088216			0.016	0.005
	29754300			0.027	0.009
	39923300			0.013	0.003
	43850215			0.018	0.004
	49599206			0.011	0.003
	64965310			0.019	0.005
	68849206			0.013	0.003
	73019200			0.010	0.002
	77750514			0.015	0.005
	79701814			0.021	0.005
	89122200			0.008	0.001
	97481706			0.016	0.005
	98956212			0.018	0.005
	152587905			0.011	0.002
	171209714			0.013	0.003
	203439500			0.013	0.003
	217553200			0.010	0.003
	242713704			0.015	0.004
	291747904			0.013	0.002
	304408700			0.023	0.007
	312500202			0.009	0.002
	314821503			0.008	0.001
	315298200			0.011	0.003
	315504300			0.015	0.003
	320462200			0.020	0.004
	321882600			0.024	0.005
	321950400			0.016	0.004
	327485900			0.013	0.003

FRACTURE_TROCHANTER_FEMALE →exceeding threshold above					
	ID PATIENT	TRABECULAR		CORTICAL	
		mean	std	mean	std
MPE	8799900			0.020	0.006
	23505027			0.019	0.005
	75004102			0.030	0.003
	79030800			0.014	0.004
	99151806			0.034	0.010
	99458007			0.023	0.007
	153229400			0.037	0.004
	176038902			0.041	0.010
	183772502			0.034	0.009
	183843600			0.017	0.004
	184256103			0.023	0.003
	268606704			0.020	0.006
	321555600			0.025	0.003
	322029601			0.023	0.003
	322806601			0.019	0.005
	322939900			0.010	0.003
	326296201			0.022	0.009
	326855900			0.021	0.003
	327569400			0.030	0.004

Appendix II

- Neck Analysis on Stress variable

NeckAnalysis			
Stress			
	1. Group	**mean**	**Std.Error**
Stress_mean	Control	46.690	1.235
Stress_mean	NeckFract	34.529	1.474
Stress_std	Control	24.611	0.740
Stress_std	NeckFract	19.554	0.883

NeckAnalysis			
Stress			
	2. Tissue	**mean**	**Std.Error**
Stress_mean	Trab	15.506	0.559
Stress_mean	Cort	65.713	1.552
Stress_std	Trab	12.314	0.340
Stress_std	Cort	31.851	0.850

- Trochanter Analysis on Stress variable

TrocAnalysis			
Stress			
	1. Group	**mean**	**Std.Error**
Stress_mean	Control	75.835	2.825
Stress_mean	TrocFract	48.379	3.942
Stress_std	Control	43.791	1.557
Stress_std	TrocFract	31.029	2.173

TrocAnalysis			
Stress			
	2. Tissue	**mean**	**Std.Error**
Stress_mean	Trab	16.410	0.645
Stress_mean	Cort	107.804	4.287
Stress_std	Trab	10.937	0.371
Stress_std	Cort	63.883	2.323

- Trochanter Analysis on Strain variable

TrocAnalysis			
Strain			
	1. Group	**mean**	**Std.Error**
Strain_mean	Control	0.017	0.001
Strain_mean	TrocFract	0.018	0.001
Strain_std	Control	0.008	0.000
Strain_std	TrocFract	0.007	0.001

TrocAnalysis			
Strain			
	2. Reduced_Increased	**mean**	**Std.Error**
Strain_mean	RedVar	0.016	0.001
Strain_mean	IncrVar	0.020	0.001
Strain_std	RedVar	0.011	0.000
Strain_std	IncrVar	0.005	0.000